

AN ABSTRACT OF THE THESIS OF

JOHN WILLIAM KAAKINEN for the MASTER OF SCIENCE  
(Name) (Degree)

in CHEMICAL ENGINEERING presented on August 30, 1967  
(Major) (Date)

Title: A MATHEMATICAL MODEL FOR DIFFERENTIAL THERMAL  
ANALYSIS

Redacted for Privacy

Abstract approved: \_\_\_\_\_  
R. V. Mrazek

A mathematical model of a differential thermal analysis (DTA) system was formulated so that influence of the various physical parameters on the DTA peak could be determined. The specific DTA apparatus simulated had cylindrical sample holes drilled into a nickel block considered to have a negligible thermal resistance, and the specific reaction was the  $\alpha$  to  $\beta$  quartz crystal transformation with zero-order kinetics. For this specific DTA system the thermal resistance of the sample was the controlling factor causing the differential temperature; consequently, the model was sublimated to a heat transfer problem involving a moving phase boundary within a cylinder being heated. The ordinary explicit finite difference method was adapted to describe the temperature profile in an infinite-cylindrical sample, and special equations were derived to consider the moving phase boundary. A digital computer solution of these equations produced

graphical DTA peaks whose shape was largely dependent upon the values of the governing physical parameters for the apparatus and the samples.

The results compared well with previous theoretical investigations of a differential thermal analyzer, and it is felt that the results of this study are more accurate than those obtained by other investigators. In addition, good qualitative agreement was found between the results of the present model and the experimental peaks of the two previous investigations of the  $\alpha$ - $\beta$  phase transformation in quartz. Theoretical variations in the heating rate generated the same general trends in the maximum peak temperature and the peak area as indicated by previous experimental results. Finally, the effects of the heat of transformation and thermal diffusivity on the shape of the DTA peak were determined.

Recommendations for the application of this model to a two-dimensional case are made for a cylinder. Specifically, a procedure for treating the movement of a phase boundary of variable shape is suggested.

A Mathematical Model for Differential  
Thermal Analysis

by

John William Kaakinen

A THESIS

submitted to

Oregon State University

in partial fulfillment of  
the requirements for the  
degree of

Master of Science

June 1968

APPROVAL:

Redacted for Privacy

---

Professor of Chemical Engineering

in charge of major

Redacted for Privacy

---

Head of Department of Chemical Engineering

Redacted for Privacy

---

Dean of Graduate School

Date thesis is presented

August 30, 1967

Typed by Clover Redfern for

John William Kaakinen

## ACKNOWLEDGMENT

I wish to thank the many people who contributed to the completion of this thesis; I would like to list some of them by name:

Dr. R. V. Mrazek for the initial ideas for the topic of this thesis, for his valuable suggestions throughout the course of the theoretical work contained in this thesis, and for his constructive criticism of the writing of this thesis.

The Oregon State University Computer Center, Dr. D. D. Aufenkamp, Director, for contributing financial support (National Science Foundation Grant GP 5769) in the form of computer time, which made this project possible.

Mr. Jack White of the Albany Metallurgy Research Center, U. S. Bureau of Mines, for the numerous suggestions and information upon the practical aspects of DTA.

The Chemical Engineering Department, Prof. J. S. Walton, Head, which generously contributed the use of its facilities.

Mrs. Louise Rainey and Miss Karen Tsubota, for their assistance in typing the rough draft.

Mr. Martin Ludwig for his invaluable help, including many suggestions which contributed to improving the clarity and the readability of the writing in this thesis.

The people of the State of Oregon for their many tax dollars which have contributed to my formal education.

## TABLE OF CONTENTS

	Page
INTRODUCTION	1
BACKGROUND AND THEORY	3
Differential Thermal Analysis	3
Peak Shape	4
Uses of DTA	6
The DTA Process	7
Aspects of the Apparatus	8
Heat Conduction in the Samples	9
Other Physical Aspects	12
Previous Mathematical Treatments	12
Peak Area and Latent Heat	13
Reaction Kinetics Parameters	15
Theoretical DTA Peaks	17
The Peaks of Smyth	18
The Peaks of Tsang	21
Moving Boundary Problems	24
Summary of Previous Models	26
THE DTA MODEL	28
A DTA System	29
Assumptions and Basic Equations	33
The Finite Difference Method	42
Criteria for Selection	44
Explicit Methods	46
The Boundary Equations	51
Three-point Equations	53
Two-point Equations	56
Special Cases	59
The Digital Computer Solution	63
RESULTS AND DISCUSSION	66
Comparison with Previous Results	66
Sample Properties and Peak Shape	74
CONCLUSIONS	78
RECOMMENDATIONS FOR FUTURE WORK	79
BIBLIOGRAPHY	81
APPENDIX	86

	Page
Appendix I	86
Nomenclature	87
Appendix II	90
Two Explicit Finite Difference Methods	91
Appendix III	94
Computer Programs	95
Appendix IV	101
A Finite-Length Cylindrical Sample	102
Appendix V	107
Thermocouple Effects	108

# A MATHEMATICAL MODEL FOR DIFFERENTIAL THERMAL ANALYSIS

## INTRODUCTION

Differential thermal analysis (DTA) can be used to study heat effects which accompany a phase change, and to determine the temperature at which an abrupt phase change occurs. This use of DTA allows a tremendous reduction in the effort and time required to measure these phase change temperatures (melting points, boiling points, and structure transformation temperatures) over the usual methods. (Accurately determining a transition temperature using vapor pressure or heat capacity measuring techniques takes time in the order of days, but a DTA peak can be generated in about an hour.) Accurate melting points and boiling points have been determined (2, 45) using a specially designed DTA apparatus, but this determination using normal DTA apparatus has been inaccurate because the correspondence between specific points along the peaks generated by a differential thermal analyzer and the temperatures of interest has been unclear (15, p. 154-159).

The reason for this lack of clarity in the precise evaluation of DTA peaks is the lack of understanding of the processes which cause the shape of a DTA peak (15, p. 152-154). Since DTA is an empirically developed method (29), theoretical considerations have seriously



lagged the applications (37, p. 1-13). In fact, no one has quantitatively described the many variables affecting a peak or mathematically generated an accurate DTA peak for comparison with any experimental case, although some have generated theoretically qualitative peaks (38, 45). The accurate quantitative description of the process involved in DTA is necessary before precise quantitative measurements of thermal properties can exist and before the wide range of interpretations and unsubstantiated assumptions used by various investigators can be resolved. It is important to mention that an important reason why an accurate solution may not have been found previously is that few fast digital computers needed to determine the numerical solution of the model, have been available.

The present work was proposed to investigate the relationship between the physical variables which cause the shape of the DTA peak. Specifically, the main purpose of this work is to formulate a mathematical model of a differential analyzer capable of producing an accurate DTA peak. It is hoped that a comparison between the peaks of this model and peaks derived from experimental means will promote a greater understanding of the relationships between the physical variables causing the peak. As a result, it is hoped that the accurate measurements of certain thermal quantities from DTA peaks will be possible.

## BACKGROUND AND THEORY

### Differential Thermal Analysis

The method of differential thermal analysis (DTA) measures heat effects that occur when a substance is heated. Such heat effects are caused by any absorption or evolution of heat which is anomalous to that described by a normal heat capacity. These effects are usually heats of physical transitions or heats of chemical reactions (49, p. 132), and the amount of heat evolved in one of these changes must be large enough to be plainly detected by the differential thermal analyzer. The temperature range and the rate of occurrence of such a phase change varies depending upon the reaction kinetics. The phase change can occur instantaneously at a specific temperature (normal melting of ice) or contrastingly, it can occur gradually over a wide temperature range (the dehydration of a clay material).

A differential thermal analyzer (15, p. 107-148, p. 13-40, p. 186-228) compares the temperature in the center of the sample with the temperature in the center of a reference material when the materials are heated together at a uniform rate. The two substances are placed into a sample holder (usually cylindrical holes of equal size symmetrically drilled into a metal block) contained inside the furnace of the analyzer, and the constant rate of temperature increase of the sample holder is maintained by a temperature controller. The

reference material, which should ideally have a thermal diffusivity equal to that of the sample, must not have a phase change in the temperature range of interest; in other words, it must be thermally inert in this temperature range. The difference in temperature is measured by a differential thermocouple, one branch placed within the sample and the other branch placed within the inert material. The emf of this differential thermocouple plotted by a recorder against time or against an emf of some other thermocouple in the system gives a thermogram characteristic of the sample and subject to experimental variables. Various investigators have used system thermocouples which measured the temperature in the sample, in the reference material, or in the metal block (3).

### Peak Shape

The shape of a thermogram peak can be more meaningful if it is heuristically explained. A comparison between the differential temperature  $\Delta T$ , and the temperatures of the sample, of the reference material, and of the block is shown in Figure 1. Both substances are heated at a uniform rate maintained in the metal block. A quasi-steady state profile exists in the substances at a sufficient time after the heating begins. At this stage the differential temperature, the difference between the temperatures of the inert substance and of the sample, is constant providing the thermal diffusivities of

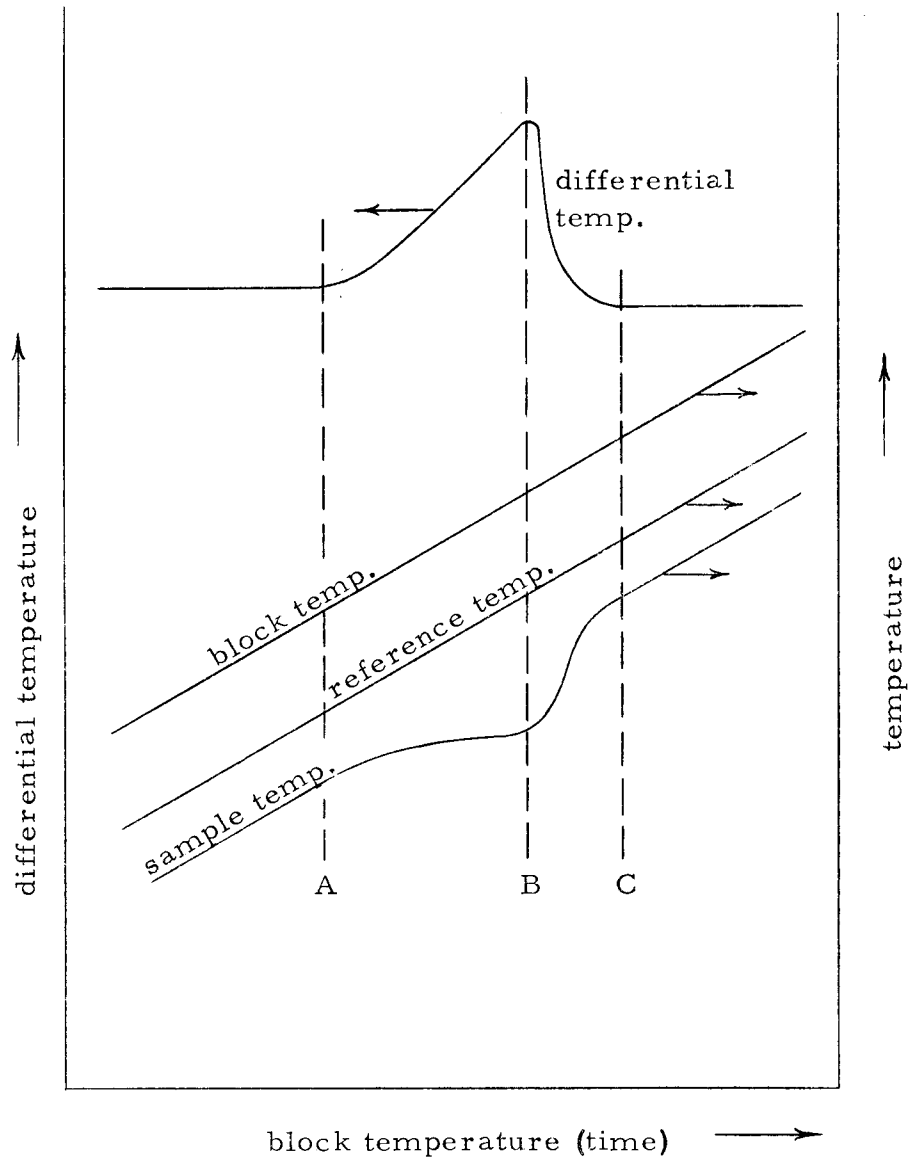


Figure 1. The differential temperature and various system temperatures during a DTA process. A. Reaction beginning. B. Reaction completed. C. Quasi-steady state profile in sample re-established.

the substances are constant or change proportionately, and this constant value of  $\Delta T$  provides a baseline on the thermogram. Since the diffusivity of the reference material remains nearly constant throughout the DTA process, it will be said to maintain a profile of constant shape. As an endothermic transition begins at the surface of the sample at point A, a sharp decrease of the heat transfer to the center occurs. Between A and B the inside of this sample is heated more slowly than the reference material causing the upward deflection of the differential temperature. As the transition approaches completion at B the peak reaches a maximum, but upon completion of the transition, the return to a quasi-steady state profile in the sample between B and C causes  $\Delta T$  to decay. At C the profile in the sample is again invariant, and the values of  $\Delta T$  at A and at C will be the same if the diffusivity of the sample does not change during the reaction. If a change in the sample diffusivity does occur, the baseline at C will be shifted from that at A.

### Uses of DTA

The number, location, and nature of the DTA peaks can be used to characterize the sample. Consequently, DTA has applications in qualitative and quantitative studies in ceramics, metallurgy, geology, mineralogy, soils, and chemistry. Specifically, the peaks can be used to identify a substance. Literally thousands of different

substances have been tested using DTA (37, p. 571-618), but unfortunately, the data obtained by one experimenter often cannot be used for direct comparison by another experimenter because of the wide variation in apparatus and techniques (1). In addition, quantities which investigators obtained from a DTA peak have included the amount of reactive component in a mixture (43), the detection of a phase change temperature (46), and the heat of reaction (47). The kinetic mechanisms of reactions have also been determined from these peaks (6, 22). The results of these quantitative studies have been accurate in some investigations and erroneous in many other investigations, but while DTA is not generally as accurate as some other quantitative methods, it is sometimes the only simple method which can be used (29). However, DTA has been used most successfully as a qualitative or semiquantitative tool (15, p. 1-52). A major reason for this variability in the quantitative accuracy of DTA is the lack of precise theoretical knowledge of the variables affecting peak shape.

### The DTA Process

A complete theoretical model of a DTA apparatus must take into account numerous physical aspects. These aspects include the heat transfer characteristics of the system, the kinetics of the phase changes, the diffusion of any gaseous reaction products, the

thermocouple effects, the temperature control, the variation of physical and chemical properties of the samples and the sample holders during the process, and any effect of the gaseous atmosphere (1). It is obvious that the complexity of a completely general model that would consider all types of chemical and physical phase changes and all variations in apparatus makes such a model improbable. Instead, models describing particular types of apparatus and of reactions are more reasonable, and this less general approach has been followed by the previous work and will also be followed by the present work.

#### Aspects of the Apparatus

The aspects of the heat transfer, the temperature control, and the thermocouple effects are determined largely by a specific apparatus with the notable exception of heat transfer in the samples. Sample holder characteristics have a tremendous effect upon the proper mathematical treatment of the heat transfer (5). This effect is not only in the size of the sample wells but also in the geometry and material of the holder. On the one hand a sample holder can be made out of a metal block which has negligible thermal resistance to heat flow in comparison to the samples (42), or on the other hand the sample holder can have such a high resistance that the temperature gradient in the samples can be neglected (47). The temperature control is normally achieved by an electronic system which attempts to cause

the block temperature to rise at a constant rate, the accuracy of this constant rate being dependent upon the apparatus. The assumption that the block continues rising at a constant rate throughout the process (an assumption made by all theoretical papers) could be erroneous particularly if the heat effect is large in comparison to the total heat capacity of the block. This error is caused by the lag present in most temperature controllers. In addition to these other apparatus variables, the finite heat capacity of the thermocouples and the heat conduction along the thermocouple wires could have a significant effect (5).

#### Heat Conduction in the Samples

In order to specifically describe the heat transfer aspect within the samples the heat conduction equation is used. The fundamental heat conduction equation (7, p. 1-13; 12, p. 9-11; 24, p. 70-73) for a homogeneous solid with a constant thermal conductivity is

$$\rho c \frac{\partial T}{\partial t} = k \nabla^2 T \quad (1)$$

where  $\rho$  = the density,

$c$  = the heat capacity per unit mass,

$k$  = the thermal conductivity,

$T$  = temperature,

$t$  = time,

and  $\nabla^2$  = the Laplacian operator.



The Laplacian operator in cartesian coordinates,  $x, y, z$ , is

$$\nabla^2 = \frac{\partial^2}{\partial x^2} + \frac{\partial^2}{\partial y^2} + \frac{\partial^2}{\partial z^2} \quad (2)$$

and in cylindrical coordinates,  $r, \theta, z$ , is

$$\nabla^2 = \frac{1}{r} \frac{\partial}{\partial r} + \frac{\partial^2}{\partial r^2} + \frac{1}{r^2} \frac{\partial^2}{\partial \theta^2} + \frac{\partial^2}{\partial z^2} . \quad (3)$$

For one dimensional parallel heat flow in a slab the heat equation can be simplified to

$$\rho c \frac{\partial T}{\partial t} = k \frac{\partial^2 T}{\partial x^2} , \quad (4)$$

and for only radial flow in a cylinder the heat equation can be simplified to

$$\begin{aligned} \rho c \frac{\partial T}{\partial t} &= k \frac{1}{r} \frac{\partial}{\partial r} \left( r \frac{\partial T}{\partial r} \right) \\ &= k \left( \frac{\partial^2 T}{\partial r^2} + \frac{1}{r} \frac{\partial T}{\partial r} \right) \end{aligned} \quad (5)$$

Analytical solutions for the heat equations exist for certain geometries when the surface of a homogeneous medium is being increased at a rate such that  $T = \phi t + T_0$ , where  $\phi$  and  $T_0$  are constants, and the density, conductivity, and specific heat capacity are constant. These solutions are available, in general, for cases

where no phase change occurs. For the case where this heating has begun at  $t = 0$  with a temperature profile uniformly equal to zero, a solution for Equation 5 in an infinite cylinder of radius  $a$ , is given by Carslaw and Jaeger (7, p. 201) as

$$T = \phi\left(t - \frac{a^2 - r^2}{4\alpha}\right) + \frac{2\phi}{a\alpha} \sum_{n=1}^{\infty} e^{-\alpha\beta_n^2 t} \frac{J_0(r\beta_n)}{\beta_n^3 J_1(a\beta_n)} \quad (6)$$

where  $J_0$  and  $J_1$  are Bessel functions of orders 0 and 1, respectively, and  $\beta_n$  is the  $n$ th root of  $J_0(a\beta_n) = 0$ . A solution for a finite length cylinder with these boundary conditions has been given (51) and also for unidirectional flow in a slab (7, p. 104). After a sufficiently long time after heating begins, a quasi-steady state profile can be described for unidirectional heat flow (45) in the  $x$  direction of a slab of thickness  $2l$ , by

$$T = T_o + \phi\left(t - \frac{l^2 - x^2}{2\alpha}\right), \quad (7)$$

and in the radial direction of a cylinder, by

$$T = T_o + \phi\left(t - \frac{a^2 - r^2}{4\alpha}\right). \quad (8)$$

However, when thermal properties are varying or an inhomogeneous boundary condition occurs, analytical solutions are often not

possible. In these cases, approximate solutions must be used (7, p. 282-283).

### Other Physical Aspects

The aspects of the kinetics of the phase changes, the diffusion of the gaseous reaction products, and the effect of the gaseous atmosphere are largely determined by the nature of the phase change. When the phase change is a complicated reaction, such as the dehydration or decomposition of a clay material, all of these aspects are important. However, when the phase change is strictly a physical transition with no gaseous products, such as a fusion or a crystal structural transformation, only the kinetics (which are often trivial for this case) need to be considered. It can be quickly deduced from the above that a model considering a complicated chemical reaction would be much more difficult to formulate accurately than one considering a simple physical change.

### Previous Mathematical Treatments

None of the previous mathematical models have accurately predicted a DTA peak because unrealistic assumptions have been made to render the resulting equations easily solvable. There are three reasons why previous models have been generated: (1) a desire to know the relationship between the peak area and the latent heat of a

phase change, (2) a desire to know the kinetic parameters of a reaction, and (3) a desire simply to enlarge the theoretical knowledge of DTA (15, p. 152). These three types of models will be considered separately.

### Peak Area and Latent Heat

Many papers have derived and studied the relationship between the area under a thermogram peak and the corresponding latent heat. (5, 25, 35, 39, 40, 41, 47). Many of the derived expressions have the form

$$M\Delta H/gk = \int_a^c \Delta T dt \quad (9)$$

where

M = the mass of the active material in the sample,

$\Delta H$  = the specific latent heat,

k = the thermal conductivity,

g = the geometrical constant,

t = time,

$\Delta T$  = the differential temperature,

and a and c specify a time interval sufficiently large to contain all effects of the phase change.

Speil (40) used this equation to predict the composition of various clays with reasonable accuracy from thermograms, and he realized

that it was only approximate since the thermal gradients in the actual samples were neglected. Kronig and Snoodyk (25) and Boersma (5) each derived this equation with specific expressions for  $g$  for both a spherical and infinitely long cylindrical sample holder. They assumed the thermal conductivity of the block to be much greater than that of the sample so that the resistance in the block could be neglected, and they also assumed that the thermal properties of the two samples were identical except for the thermal effect in the test material. The former assumption is reasonable, but the latter is not consistent with reality as the respective conductivities, densities, and heat capacities of the inert and test materials are more often not alike. Soule (39) and Sewell and Honeyborne (35) proved that Equation 9 is general for any sample shape providing several conditions are met: (1) the boundaries of the inert and test materials are of the same shape, (2) the temperatures are measured in identical locations in the two materials, (3) the thermal resistance within the block and between the block and each sample is negligible, and (4) the heating rate is linear. The assumptions (1) and (2) are plausible, but the validity of (3) and (4) need to be verified experimentally before they should be completely accepted. Several conclusions were made from these general results (35): the peak area is independent of the heating rate, of the reaction rate, and of the specific heat of the test sample, but is dependent upon the conductivities of the test sample

and the materials in the furnace, and, of course, dependent upon the latent heat of the phase change.

Some other workers (5, 47) have derived expressions relating the reaction heat to the peak area in a different type of sample holder which has a high thermal resistance. When such a sample holder is used, the thermal resistance of the samples may be neglected, and this thermal method takes on a name different from DTA, differential calorimetry (15, p. 159-165). Vold (47) and Boersma (5) considered this type of apparatus and state that neglecting the thermal resistance of the sample allows an expression for the latent heat which contains only the heat transfer properties of the apparatus. While use of this different type of sample holder allows the elimination of the troublesome problem of considering heat lag in the samples, this method gives peaks which are much broader, and, as a result, difficulty is encountered in defining two peaks occurring close together (5). In any case, the theoretical considerations of Vold and Boersma will not apply to the most widely used type of DTA sample holder.

#### Reaction Kinetics Parameters

Papers dealing with determining reaction kinetics parameters have removed the problem of thermal lag in the samples and concentrated on kinetics affecting the DTA curve. Murray and White (31) merely neglected thermal lag when they equated temperature

difference and loss-in-weight of the sample as exactly analogous ways of following the decomposition in clay materials. Kissinger (22, 23) assumed in addition that the rate of maximum reaction occurred at the peak temperature, and he generated a DTA peak and kinetics parameters which showed good agreement with his experimental results. Borchardt and Daniels (6) changed the conditions of the experiment in order to avoid the problems of thermal lag by making the samples well-stirred liquid solutions; thus, the samples were of uniform temperature. More recent works (15, p. 210-214; 33), which reviewed the methods of Kissinger and of Borchardt and Daniels, found the method of Borchardt and Daniels to give accurate predictions and the well-accepted method of Kissinger to be seriously in error. It was believed that in Kissinger's original work the error of neglecting thermal lag was cancelled out by the error in another assumption, namely, that the maximum reaction rate occurs at the peak of the DTA curve, so that for certain specific substances and conditions the DTA curves generated by Kissinger's equations may agree with experimental ones. Thus, thermal lag effects can be eliminated by changing the experiment (such as using well-stirred liquid samples rather than a solid material), but with normal DTA equipment the incorporation of the sample's temperature gradient is necessary for accuracy. At this time, this correction has not been published.

### Theoretical DTA Peaks

Several authors have attempted to enlarge upon the theoretical knowledge of DTA. Smyth (38) and Tsang (45) theoretically generated DTA peaks which elucidated the qualitative nature of experimental peaks. Smyth's work is the most original and complete general description of the heat transfer aspect within DTA samples published to date. Smyth uses a finite difference method to follow a moving phase boundary in a slab. Tsang's work follows that of Smyth by describing an alternative mathematical method for generating the same type of DTA peak.

Both investigators made the following stipulations about the hypothetical DTA system they were describing: (1) the thermal conductivities, densities, and specific heat capacities (other than the heat effect in the test sample) in both materials, which are assumed to be homogeneous, are equal and constant throughout the process, (2) the reaction was endothermic, free of any reaction products, and zero order, instantaneously occurring at one distinct transition temperature, (3) the heating rate at the surfaces of the samples is linear with time, and (4) the heat conduction occurs principally in one coordinate direction in a slab (Smyth and Tsang) or in a cylinder (Tsang). From stipulations (1), (3), and (4) the quasi-steady state profile in the inert sample remains invariant throughout the process according



to Equations 7 and 8. An analytical solution of the heat equation under these conditions is impossible (7, p. 282-283) because of the phase change so that approximate numerical methods are needed, and the methods used by Smyth and by Tsang will be considered separately.

The Peaks of Smyth. Smyth (38) found the temperature profile in the slab-shaped sample by solving the heat equation using a numerical method attributed to Schmidt (28, p. 43-51). Smyth divided the slab by parallel planes normal to the direction of heat flow  $\Delta x$  cm. apart and defined a time interval

$$\Delta t = \frac{(\Delta x)^2}{2a} \text{ seconds} \quad (10)$$

where  $a$  is the diffusivity. This Schmidt method states that the temperature at time  $t$  on a grid line is equal to the mean of the temperatures at time  $t - \Delta t$  on the two adjoining grid lines. This method does not account for the phase change, so Smyth generated additional equations.

Smyth derived finite difference equations to describe a moving phase boundary from a heat balance about the boundary. The temperature profile and this boundary at some time during the transition are shown in Figure 2, together with the temperature gradients at the

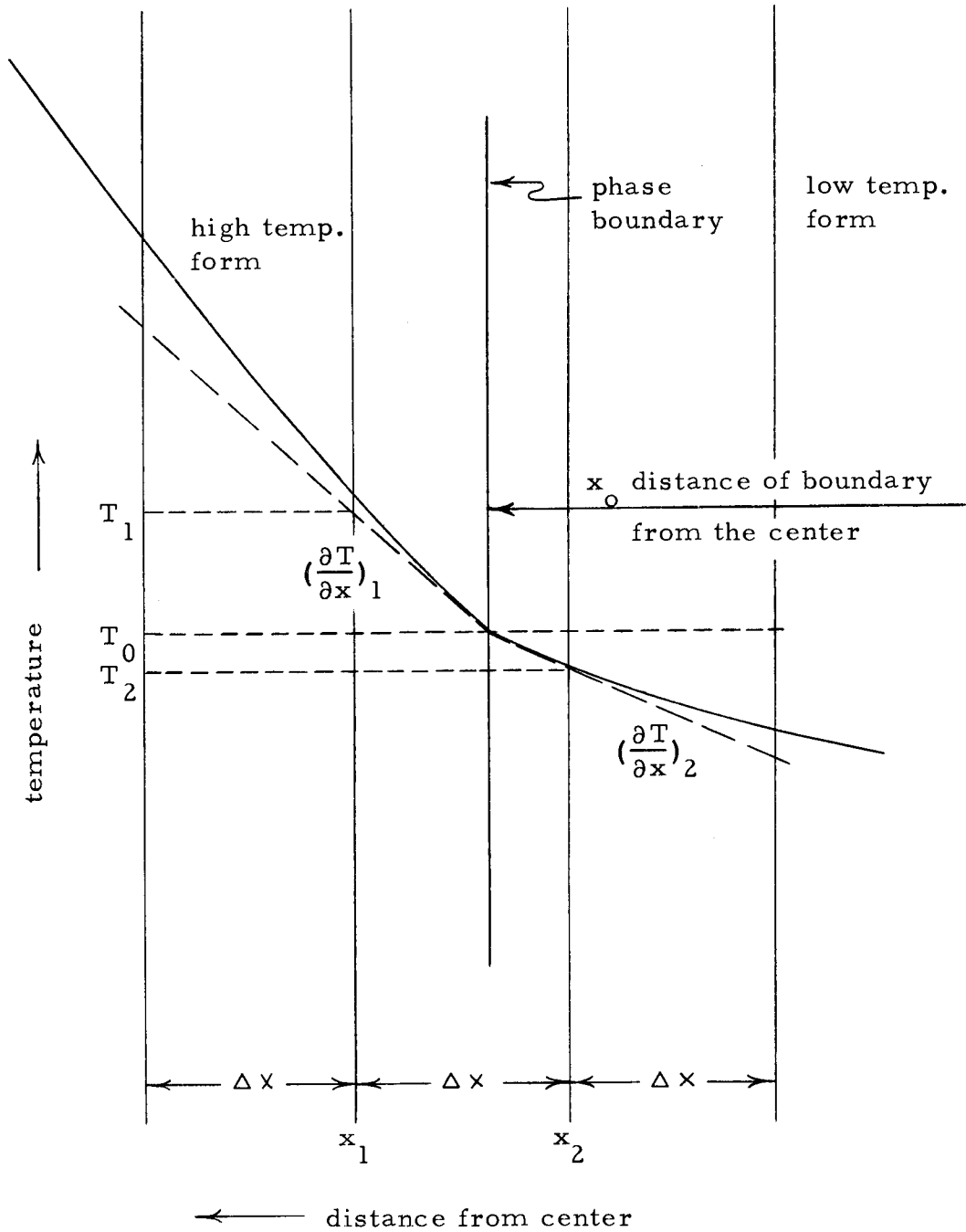


Figure 2. Diagram used by Smyth (38) to calculate the phase boundary movement within a slab.

boundary,  $(\frac{\partial T}{\partial x})_1$  and  $(\frac{\partial T}{\partial x})_2$ , in the high and low phases, respectively. If the heat of transition per unit mass is  $\Delta H$ , the movement  $\delta x$  cm., of the boundary in a time interval  $\Delta t$  was derived from a heat balance as

$$\delta x = \frac{1}{\rho \Delta H} [-k(\frac{\partial T}{\partial x})_1 + k(\frac{\partial T}{\partial x})_2] \Delta t \quad (11)$$

where  $\rho$  and  $k$  are the density and thermal conductivity, respectively. The term in brackets can be interpreted as the net rate of heat conduction into the boundary, which converts a thickness,  $\delta x$ , of material in the low form to the high form in a time interval  $\Delta t$ . Since the gradients cannot be found directly the following approximations were used:

$$(\frac{\partial T}{\partial x})_1 \cong \frac{T_1 - T_0}{x_1 - x_0} \quad \text{and} \quad (12)$$

$$(\frac{\partial T}{\partial x})_2 \cong \frac{T_0 - T_2}{x_1 - x_0} \quad (13)$$

where the  $T$ 's and  $x$ 's are shown in Figure 2.

The Schmidt method and the equation determining the boundary movement were combined, and iterative calculations across the slab at intervals of  $\Delta t$  seconds described the temperature profile and the boundary movement within the slab being heated. This method was applied to generating a DTA peak as follows: the temperatures

of the center of the slab were calculated using this method, the temperatures of the center of an inert slab material were found from Equation 7, and the differences of these center temperatures were plotted against a reference temperature to give a simulated DTA peak. The resulting DTA peaks had three shapes, depending upon whether the reference temperatures were chosen in the inert material, in the block (corresponding to the time for a constant heating rate), or in the sample. The case for the reference temperature in the inert material is shown in Figure 3. The peak for the case of the reference being in the block has a similar shape except that the entire peak is shifted along the temperature axis so that the initial deviation from the baseline corresponds to the transition temperature. When the center of the test sample is the location of the reference temperature, a completely different shape results, the peak rising very sharply and the temperature at the top of the peak corresponding to the transition temperature. These peaks and the related discussions of Smyth are the clearest and most complete qualitative description of DTA peaks heretofore published. However, Smyth's work had no intention of quantitatively predicting experimental DTA curves.

The Peaks of Tsang. The mathematical method used by Tsang (45) utilized several assumptions which allowed the solution to be

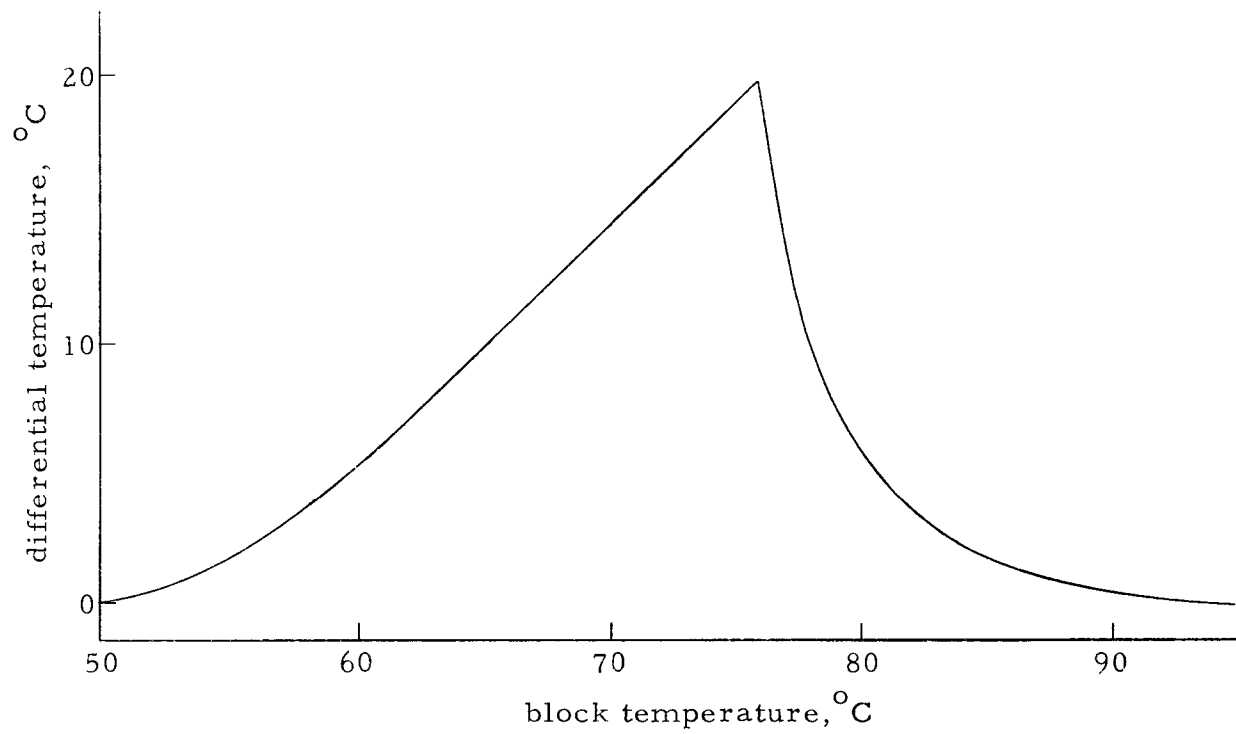


Figure 3. Theoretical DTA peak of Smyth (38) for a slab-shaped sample.

obtained without the large number of numerical steps required by Smyth's method. Tsang treated the sample as a system made up of two hypothetical materials, one material  $a$ , having a finite  $k$  and having a  $C$  and a  $\Delta H$  equal to zero and the other material  $b$ , having a  $k$  equal to infinity and a positive  $C$  and a positive  $\Delta H$ . The material  $b$ , can be considered negligibly thick as regards heat transfer because there is no resistance to heat transfer, but the thermal inertia must be considered. The material  $a$ , has no thermal inertia but offers a resistance to heat flow; thus, the heat transfer problem is sublimated to one of flow through a material  $b$ , between points of material  $a$ , being heated. The size and location of the layers of  $b$  is determined by two conditions: first, that the rate of temperature rise upon heating varies linearly with position, and second, that the sum of the volumes of the layers is equal to total volume of the actual sample. The equivalent conductivity of material  $a$  for heat transfer between layers of  $b$  was determined by application of the solution 7 for the heat equation. By using this equivalent system of materials  $a$  and  $b$  and normal techniques for solving ordinary differential equations, Tsang obtained relatively simple solutions for one and two segments in a slab which agreed remarkably well with Smyth's curve shown in Figure 3. Tsang also applied his method to the infinite cylindrical shape for one and two sections (see Figure 7).

### Moving Boundary Problems

While Smyth considered a moving boundary in DTA, many mathematical works have considered a moving boundary in melting problems, often called Stefan problems, (11, 44). These methods may be applied to the moving boundary in a DTA sample. Unfortunately, none of these solutions have included the linearly rising surface temperature boundary conditions nor the geometry of a cylindrical material; however, the application of ideas from these works is possible. For example, in treating a moving boundary within a slab Crank (9) described the boundary movement and the temperatures at grids close to the boundary by using finite difference equations for the first and second distance derivatives of temperature derived from Lagrange's three-point interpolation formula (26, p. 36-41; 30, p. 83-92). This idea of applying Lagrange's three-point formula to a moving boundary problem will be applied to a cylinder in the present work.

Lagrange's interpolation formula, which can treat unequally spaced functions such as are encountered in a moving boundary problem, can be written as

$$f(x) = \sum_{j=0}^n l_j(x)f(a_j) \quad (14)$$

where

$$l_j(x) = \frac{p_n(x)}{(x-a_j)p'_n(a_j)} \quad (15)$$

and

$$p_n(x) = (x-a_0)(x-a_1)\dots(x-a_{n-1})(x-a_n) \quad (16)$$

For three point formulas ( $n=2$ ) this becomes

$$f(x) \approx \frac{(x-a_1)(x-a_2)}{(a_0-a_1)(a_0-a_2)} f(a_0) + \frac{(x-a_0)(x-a_2)}{(a_1-a_0)(a_1-a_2)} f(a_1) + \frac{(x-a_0)(x-a_1)}{(a_2-a_0)(a_2-a_1)} f(a_2), \quad (17)$$

and after taking the first and second derivatives the results are

$$\begin{aligned} \frac{df(x)}{dx} &\approx \frac{(x-a_1)+(x-a_2)}{(a_0-a_1)(a_0-a_2)} f(a_0) + \frac{(x-a_0)+(x-a_2)}{(a_1-a_0)(a_1-a_2)} f(a_1) \\ &\quad + \frac{(x-a_0)+(x-a_1)}{(a_2-a_0)(a_2-a_1)} f(a_2) \end{aligned} \quad (18)$$

and

$$\frac{d^2f(x)}{dx^2} \approx 2 \left[ \frac{f(a_0)}{(a_0-a_1)(a_0-a_2)} + \frac{f(a_1)}{(a_1-a_0)(a_1-a_2)} + \frac{f(a_2)}{(a_2-a_0)(a_2-a_1)} \right] \quad (19)$$

Thus, Crank (9) used expression 18 to calculate a temperature gradient and expression 19 to calculate the right side of the heat Equation 4 for a slab with unidirectional heat flow.

Similarly, equations for a cylinder can be obtained from 18 and 19. In a cylinder the Laplacian has the form given by Equation 3, and



considering only heat flow in the radial direction, the right side of the heat Equation 5 can be written as

$$\frac{d^2 T(x)}{dx^2} + \frac{1}{x} \frac{dT(x)}{dx} \cong 2 \left[ \frac{T(a_0)}{(a_0 - a_1)(a_0 - a_2)} + \frac{T(a_1)}{(a_1 - a_0)(a_1 - a_2)} + \frac{T(a_2)}{(a_2 - a_0)(a_2 - a_1)} \right] + \frac{1}{x} \left[ \frac{(x - a_1) + (x - a_2)}{(a_0 - a_1)(a_0 - a_2)} T(a_0) + \frac{(x - a_0) + (x - a_2)}{(a_1 - a_0)(a_1 - a_2)} T(a_1) + \frac{(x - a_0) + (x - a_1)}{(a_2 - a_0)(a_2 - a_1)} T(a_2) \right]. \quad (20)$$

In addition, the equations for the gradients at the phase boundary within a cylinder are identical to those within a slab. Equations 18 and 20 will be applied to the present model.

#### Summary of Previous Models

Several conclusions were made on the previous theoretical works about their usefulness in generating a DTA peak. The models which related peak area to latent heat are not applicable because they are concerned with a different area of DTA. The models which treat kinetics did not account for thermal lag, and therefore, the use of these kinetic models, such as that of Kissinger, will not give reliable results and will not give an accurate result unless a fortuitous set of conditions are used which by chance balance out unreal assumptions. The works of Smyth and Tsang give useful qualitative results but

weren't intended to give accurate quantitative results. In summation, none of these previous workers have generated a quantitative DTA model capable of predicting an experimental peak.

## THE DTA MODEL

The only two previous studies that have generated theoretical DTA peaks were qualitative rather than quantitative, and both of these use the same data and assumptions. Also, while the finite difference method used by Smyth is probably accurate, there is no assurance that Tsang's mathematical method is really accurate for the cylinder. It was intended that the present model would be an improvement over these two previous models, for the present model would attempt to predict an experimental DTA peak by using assumptions as close as possible to physical reality and by using an accurate method of numerical solution.

The development of the present model had several phases. First, a specific DTA apparatus was chosen as a basis for the model, and simultaneously, a certain type of kinetic reaction was chosen which described an instantaneous phase change. Afterwards, actual materials were chosen for both the reference sample and the test sample so that the results could be compared to the experimental observations of other workers. Second, basic mathematical equations were developed and assumptions tentatively were made which were as close to physical reality as was feasible, but for which a mathematical solution was still possible. Third, various numerical methods for solving the heat transfer equation were investigated, and the most

advantageous of these methods was chosen. Fourth, specific finite difference equations were derived for an infinite cylinder which could describe the moving phase boundary. Fifth, a computer program was written employing the difference equations to obtain numerical and graphical solutions of the model. Lastly, the numerical results were compared with other theoretical results and with experimental results. This step served as a basis for determining the validity of the model, for affecting changes in the model, and for making suggestions for future work by others on this model or a new model.

#### A DTA System

As the first step toward generating the mathematical model a specific differential thermal analyzer will be asserted as a basis for analysis, and it will be based upon a typical, commonly available apparatus, the Deltatherm model D2000 differential thermal analyzer and the Deltatherm model D2200 rate controller.<sup>1</sup> In this apparatus, diagrammed in part in Figure 4, the samples are held by holes 1/4 inch in diameter drilled 1/2 inch deep into a heavy nickel block, and a metal lid fits tightly over the holes. The system temperature measurements for the temperature controller and for the temperature axis of the thermogram, are taken in the metal block. The temperature

---

<sup>1</sup>An apparatus of this type is located at the Bureau of Mines in Albany, Oregon.

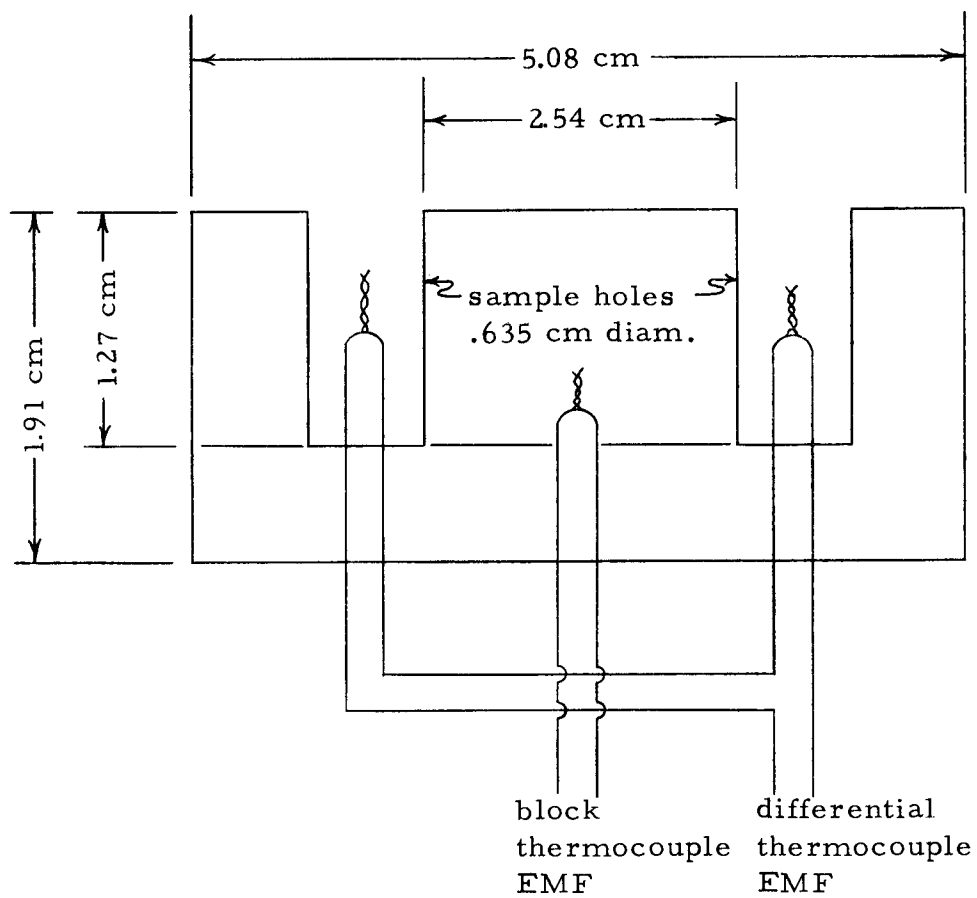


Figure 4. Diagram of the sample block and the thermocouples of the present model.

controller attempts to maintain a set rate of temperature rise in the block, but because of a high thermal inertia in the system, a relatively long time is required to affect a significant change in heat flux to the block after a command is given by the controller. There are some inertial effects and some conductance effects from the differential thermocouple located in the centers of the samples. The emf measured by the differential thermocouple, an indication of the temperature difference between the test sample and the reference sample, is illustrated by a strip-chart recorder against block temperature. Closely related to the apparatus is the reaction which generates the heat effect.

The type of reaction decided upon is a zero order, instantaneous phase change, which would occur at a specific temperature and have no gaseous reaction products. The reasons for this choice are first, that it approximates the change which occurs in many actual phase transitions, and second, that the problem of kinetics in such a reaction are trivial. The treatment of kinetics in this reaction is simple because the speed of this type of phase change is controlled only by the rate at which heat can be supplied to the material in transition. The specific heat capacity of this type of material is a fairly smooth function except precisely at the transition temperature where it has a value of infinity, and the area under the heat capacity versus temperature curve at the point of the transition temperature is equal

to the latent heat of phase transformation,  $\Delta H$ . Alternatively, this heat capacity mathematically can be considered to undergo a jump discontinuity, without this jump to an infinite value, but with the effect of  $\Delta H$  superimposed upon it at the transition temperature.

In quartz the  $\alpha$  to  $\beta$ , low form to high form, crystal structure transition has the phase change characteristics listed above (1), and therefore, quartz was chosen as the specific material to be considered. Since this phase change in quartz occurs with only a slight structural change, no extra products are formed, and only minimal changes in physical properties occur as a result of the transition.

The only significant change reported in the literature (16, p. 195) is in the heat capacity which has a value of  $0.297 \frac{\text{cal}}{\text{g}^\circ\text{K}}$  before the transition ( $\alpha$ ) and a value of  $0.267 \frac{\text{cal}}{\text{g}^\circ\text{K}}$  after the transition ( $\beta$ ).

The latent heat of the transformation is 290 calories per gram mole (50, p. 103), which is sufficiently large to produce a substantial peak, and this transition occurs at 574 degrees centigrade (50, p. 103).<sup>2/</sup>

The quartz sample was taken as crushed (100 mesh with an apparent density of  $1.358 \frac{\text{g}}{\text{cm}^3}$ <sup>3/</sup>), rather than a single crystal.

---

<sup>2/</sup>It should be mentioned that these values of properties for quartz are only approximate since variations in the transition temperature occur among different samples and even occur at different locations within a single crystal (21).

<sup>3/</sup>The properties of such a crushed quartz sample were determined in studies at the U.S. Bureau of Mines in Albany, Oregon.

The specific reference material chosen was powdered-Alumina,  $\text{Al}_2\text{O}_3$ . It is widely used in DTA (48) because of its thermal stability and its lack of a heat effect over a wide temperature range, and its use in the present model is entirely satisfactory. Having chosen the sample materials and the hypothetical apparatus, the next step was to formulate the equations and to consider applicable assumptions.

### Assumptions and Basic Equations

In order to generate a DTA peak consistent with experimental results, the mathematical model should be able to describe the physical reality of the process. The ideal mathematical model would be consistent with reality: to specify a sample geometry consistent with actual sample shapes, to account for thermal properties which change during the DTA process, to account for thermocouple effects, to specify the temperature profiles in the samples and in the block, to describe mathematically the response of the temperature controller, to realize accurately all effects of the reaction, and finally to have the accurate data necessary for describing the specific apparatus and samples for which the peak is to be simulated. However, the precise descriptions of some physical processes and the precise values of some of the physical properties presently are not known. This lack of knowledge, together with the mathematical complexities that would arise, make certain assumptions necessary.



A number of simplifying assumptions will be tentatively asserted, subject to possible change. These assumptions first will be stated and then their validity will be discussed. (1) The geometry of the sample holder will be that of a cylinder, both an infinite length cylinder with only radial heat flow and a finite length cylinder with axisymmetric heat flow. (2) The temperature gradient in the block will be negligible in comparison with the gradient in the samples. (3) The rate of temperature rise of the block will be maintained at a constant value. (4) The thermocouple effects will be neglected. (5) The thermal resistance between the block and the samples will be negligible. (6) The crushed quartz and powdered alumina will have homogeneous physical properties. (7) The thermal conductivity of quartz remains constant throughout the temperature range of the peak. (8) The reaction is zero order and occurs at one temperature, the only limitation upon its rate being the net rate of heat transfer to the reacting substance. The specific reaction which will be used is the  $\alpha$  to  $\beta$  crystal transformation in quartz. (9) The transition occurs within an infinitesimally thick boundary which separates the  $\alpha$  phase and the  $\beta$  phase of quartz. A comparison between the assumptions and this hypothetical DTA system will assess the validity of necessary assumptions.

Assumption (1), asserting a cylindrical sample geometry, is consistent with the actual sample shape. The validity of

axisymmetric heat flow lies greatly upon the validity of assumptions (3) and (6), for axisymmetric heat flow would require that the block temperature at all points in contact with the surface of the sample be equal and that the sample properties do not vary with angular position in the sample. The assumption that the cylindrical sample can be treated as infinitely long is admittedly an approximation which is a sacrifice for the sake of mathematical simplicity. The present sample has a length of twice its diameter, and assurance that an infinite cylinder is a good approximation of the present sample shape would only be possible after the finite cylinder solution had been found and shown to be nearly the same as the infinite cylinder solution.

Assumption (2) may be checked by comparison of the thermal resistance of the block and of the sample. Since the nickel block has a conductivity of  $.088 \frac{\text{cal}}{\text{sec cm } ^\circ\text{C}}$  (18, p. 2435) and the crushed quartz sample has an apparent conductivity of about  $.00589 \frac{\text{cal}}{\text{sec cm } ^\circ\text{C}}$ <sup>4/</sup>, the block conducts heat much more easily than the sample, but this higher conductive ability of the nickel is partially counteracted by the larger distances of the heat flow through the block than distances of the heat flow through the sample. The resistance of heat flow through the block is probably at least an order of magnitude less than the resistance through the sample, but it may not be completely negligible.

---

<sup>4</sup>The calculation of this value for  $k$  will be shown later in this subsection under the discussion of assumption (7).

However, it will be assumed negligible for to take it into account accurately would greatly increase the complexity of the present analysis, and a full account of the block resistance will be left for some future work for other investigators.

The validity of (3) can be checked by a comparison between the total heat capacity of the block and the heat effect of the reaction. This comparison is justified because, while the controller can maintain a constant rate of increase when gradual variations in the heat requirement occur, due to the systems relatively high heating lag it cannot respond quickly to a large abrupt change in heat flux requirements caused, for instance, by an abrupt phase change. Thus, the total energy content of the nickel block with  $c = 1.27 \frac{\text{cal}}{\text{g}^\circ\text{C}}$  (18, p. 2267) and  $\rho = 8.86 \frac{\text{g}}{\text{cm}^3}$  (18, p. 2131) and with the dimensions shown in Figure 4, is

$$\begin{aligned} \rho c V &= 8.86 \times 1.27 \times (1.905 \times 5.08 \times 5.08) \\ &= 55.0 \frac{\text{calories}}{^\circ\text{C}} \end{aligned}$$

The total heat effect of the quartz sample during a complete transition is

$$\begin{aligned} V \rho \Delta H &= \left( \pi \times \frac{.635^2}{4} \times 1.27 \right) \text{cm}^3 \times 1.358 \frac{\text{g}}{\text{cm}^3} \times \frac{290 \frac{\text{cal}}{\text{mole}}}{60.1 \frac{\text{g}}{\text{mole}}} \\ &= 8.57 \text{ calories} \end{aligned}$$

This amount of heat is the same amount required to raise the temperature of the block during heating by

$$\frac{8.57 \text{ calories}}{55.0 \frac{\text{calories}}{^{\circ}\text{C}}} = 0.156^{\circ}\text{C}.$$

Therefore, it can be said that since the heat requirement of the reaction is small in comparison to the heat supplied to the block during the process, the demanded increase in heat absorption by the heat effect will not significantly alter the heating rate.

The validity of assumption (4) will be shown later through the use of the model.

The validity of assumption (5) cannot be easily checked. However, it does seem intuitively true that the thermal contact between the sample wall and the crushed sample inside is good, and if this is true this assumption is valid.

Assumption (6) is reasonable if the correct apparent properties can be found. If the packing of the sample is done carefully as to be uniform in a particular sample and to be consistent between different samples, apparent properties which take into account the voids within the crushed samples may be used. The optimum conditions would be when actual properties for the samples are available, but since this is generally not the case, these properties usually need to be estimated.

Assumption (7) is admittedly a dangerous one, but necessary because data for the thermal conductivity,  $k$ , were not found for the  $\beta$  form of quartz. Data that were available for the  $\alpha$  form (16, p. 197) showed a large dependence upon direction of conduction through the quartz crystal, particularly at around room temperature. Since the orientation of the crystal axes would probably be random within a crushed quartz sample, the constant  $k_s$  for a solid sample was assumed to be an average of the value of  $k$  for the direction perpendicular to the crystal's  $c$ -axis and of the value of  $k$  for the direction parallel to the crystal's  $c$ -axis, thus,

$$\begin{aligned} k_s &= \frac{k_{\perp} + k_{\parallel}}{2} \\ &= \frac{.0126 + .0102}{2} \\ &= .0114 \frac{\text{cal}}{\text{sec cm } ^\circ\text{C}} . \end{aligned}$$

The apparent value for  $k$  for a crushed sample was calculated from an equation given by Smith (36) which has showed good accuracy for soils:

$$k_{\text{apparent}} = k_{\text{voids}} f + k_{\text{quartz}} (1-f)$$

where  $f$  is the void fraction calculated from the densities of the materials using

$$f = \frac{\rho_{\text{solid}} - \rho_{\text{apparent}}}{\rho_{\text{solid}}} .$$

Since the density of solid quartz is  $2.65 \text{ g/cm}^3$  (18, p. 2223) and the apparent density of the crushed sample is  $1.358 \text{ g/cm}^3$ , then  $f$  can be found;

$$\begin{aligned} f &= \frac{2.65 - 1.358}{2.65} \\ &= .487 . \end{aligned}$$

Knowing  $f$ ,  $k_s$ , and  $k_{\text{air}} = .000132 \frac{\text{cal}}{\text{cm sec } ^\circ\text{C}}$ ,  $k_{\text{apparent}}$  can be calculated as

$$\begin{aligned} k_{\text{apparent}} &= .000132 \times .487 + .0114(1 - .487) \\ &= .00589 \frac{\text{cal}}{\text{cm sec } ^\circ\text{C}} . \end{aligned}$$

This will be the constant value of  $k$  used for the quartz sample.

Under assumption (8), this type of reaction is common among simple physical phase changes such as the melting and boiling of many chemicals, and the  $\alpha \rightarrow \beta$  crystal transition in quartz (21).

Assumption (9) follows directly from assumption (8). Since the only way in which heat may be transferred through a homogeneous solid is by conduction, and since a temperature gradient is needed for conduction, the only condition where heat could be transferred through a region undergoing a zero order transition at a uniform

temperature is for that region to be infinitesimally thick.

Based upon these several assumptions, it is now possible to reasonably describe the DTA process mathematically. From assumptions (1), (2), (4), (5), (6) and (7), the only significant resistance to heat flow is in the samples, and the heat Equation 1 becomes

$$c\rho \frac{\partial T}{\partial t} = k \left[ \frac{\partial^2 T}{\partial r^2} + \frac{1}{r} \frac{\partial T}{\partial r} + \frac{\partial T}{\partial z} \right]. \quad (21)$$

When the infinite cylindrical case is considered the heat Equation 5 applies. From assumptions (2), (3), and (5) the temperature rise at the surface of the samples will be linear; mathematically this can be written as

$$T_{\text{surf}} = \phi t + T_o, \quad (22)$$

where  $\phi$  and  $T_o$  are constants.

An equation describing the movement of the phase boundary will be derived, and the result will be similar to those of Smyth (38) and Crank (9). Fourier's heat conduction law (24, p. 9) is

$$q = -kA \frac{dT}{dx} \quad (23)$$

where

$q$  = the heat flow in the direction of the gradient,

$k$  = the thermal conductivity,

$A$  = the area perpendicular to heat flow,

and  $\frac{dT}{dx}$  = the temperature gradient.

The rate of conversion for a zero order reaction can be written as

$$\frac{d(\rho V)}{dt} = \frac{q}{\Delta H} \quad (24)$$

where  $\Delta H$  is the heat of reaction per unit mass,  $\rho$  is the density of the reacting material and  $V$  is the volume of the reacting material. If the phase change occurs in a cylindrical shell of area  $A_b$ , and thickness  $S$ ,<sup>5/</sup> and if  $\rho$  is invariant with time, then  $V = A_b S$  and

$$\frac{dA_b S}{dt} = \frac{q}{\rho \Delta H} \quad (25)$$

The net heat flow through the boundary (see Figure 2) using Equation 23 is

$$q = (-k_1 A_1 \left. \frac{dT}{dx} \right|_1 + k_2 A_2 \left. \frac{dT}{dx} \right|_2), \quad (26)$$

---

<sup>5</sup>As previously stated a zero order reaction occurs within an infinitesimally thick boundary, but the finite thickness of  $S$  is introduced here to facilitate the mathematical approximations later in this paper.



and combining Equations 25 and 26 gives

$$\frac{dA_b S}{dt} = \frac{1}{\rho \Delta H} (-k_1 A_1 \left. \frac{dT}{dx} \right|_1 + k_2 A_2 \left. \frac{dT}{dx} \right|_2). \quad (27)$$

If a finite difference approximation is used for  $\frac{dS}{dt}$ , the thickness,  $\delta X$ , of material being changed during a time interval  $\Delta t$  ( $A_b$  is to be nearly constant during this time) becomes

$$\delta X = \frac{1}{A_b \rho \Delta H} (-k_1 A_1 \left. \frac{dT}{dx} \right|_1 + k_2 A_2 \left. \frac{dT}{dx} \right|_2) \Delta t. \quad (28)$$

This equation becomes precisely Smyth's Equation 11 when a infinitesimally thick boundary ( $S \rightarrow 0$ ) is used in the numerical calculations (in this case  $A_b = A_1 = A_2$ ).

### The Finite Difference Method

Since many partial differential equations and their corresponding boundary conditions do not have exact solutions, they must be solved using approximate methods, and those most commonly used are finite difference techniques. Certain other approximate methods which have been used in solving specific problems have the potential of being useful, but these methods will need to be developed further before they can be generally applied by the non-expert (14). Finite difference methods substitute difference expressions for the derivatives in a differential equation, for example

$$\left. \frac{\partial T}{\partial t} \right|_m^n = \frac{T_m^{n+1} - T_m^n}{\Delta t} + O(\Delta t) \quad (29)$$

or

$$\left. \frac{\partial T}{\partial x} \right|_m^n = \frac{T_{m+1}^n - T_{m-1}^n}{2\Delta x} + O(\overline{\Delta x})^2 \quad (30)$$

where

$\Delta t$  = the time increment,

$\Delta x$  = the distance increment,

superscript  $n$  determines a time,  $t = n\Delta t$ ,

and subscript  $m$  determines a location,  $x = m\Delta x$ .

Therefore, the problem of solving a differential equation can be reduced to an algebraic, numerical problem using finite difference techniques.

The term,  $O(\quad)$ , refers to the "order of the error" in using a particular approximation, which means that the error of one step in the calculation is proportional to the order of the particular increment as indicated. For example,  $O(\Delta t)$  means that the error decreases proportionally to a decrease in  $\Delta t$ , and  $O(\overline{\Delta x})^2$  means that the error is proportional to the square of  $\Delta x$  (26, p. 87). Since increments are less than one generally, the higher this order, the lower the error.

### Criteria for Selection

Finite difference methods are chosen according to their accuracy and to their convenience in solving a particular differential equation, and this choice varies with the equation and the boundary conditions. In considering the accuracy of a method two stipulations must be made: first, that the solution converges, which means that the finite difference solution approaches the desired analytical solution as increments become increasingly small; and second, that the solution is stable, which means that truncation errors (errors resulting from the rounding off of numbers) (26, p. 69) do not accumulate from one iteration to the next, but instead, stay of the same magnitude or preferably dampen out. Convergence can be most directly measured by comparison between the approximate solution and the analytic solution (11), if one is available, and stability can be detected operationally by noting whether the error of the solution increases and probably oscillates in sign after a number of iterations (13, p. 13). If no corresponding analytical solution is available, the best way to estimate whether or not a particular finite difference solution has converged is to calculate another solution of the problem using smaller increments, and then to compare the two solutions. If the two approximate solutions are nearly equal it can be assumed that the solution has essentially converged; otherwise smaller increments are

needed for convergence (13, p. 8-10).

It should be added that while a numerical solution may converge, this fact alone does not guarantee that the solution has converged to the solution desired, for it may have converged to an erroneous solution. A rigorous and usually very complex mathematical analysis is needed to prove the absolute convergence to the desired solution when a corresponding analytical solution is not available (11). The convergence of an explicit method for a Stefan problem has been proven (44), and since there is a close similarity between this solution of the Stefan problem and the solution of the present problem, the present explicit method will be assumed to converge to a correct solution. Comparison to experimental results will substantiate this conclusion.

Finite difference methods for solving the heat equation, which is a parabolic partial differential equation, may be dichotomized into explicit methods (12, 27) and implicit methods (10), and it was first necessary to choose one of these two types. Explicit methods have the advantage that answers at a particular time step are given in terms of known quantities, but have a disadvantage that severe stability criteria are often imposed. This means, for example, that the ratio  $\frac{a \Delta t}{\Delta x^2}$  in the case of a one-dimensional slab problem has an upper bound of 2.0, so that the time increment must be relatively small (7, p. 471; 11). Conversely, implicit methods have the advantage that they are usually unconditionally stable so that any time

increment gives a stable solution, the limitation in increment size being the convergence of the solution. However, they have the disadvantage that finding each point of a solution at a next higher time step requires the solving of a number of simultaneous algebraic equations containing other points at this next higher time step. While there are methods for finding the solutions of simultaneous equations (26, p. 163-164), the present problem would have an increased complexity over simpler heat problems due to the additional equation describing the boundary movement. Therefore, implicit methods were not considered further, and the present work was limited to the use of explicit finite difference methods.

### Explicit Methods

The first explicit method considered was the widely used conventional explicit method described by Schneider (34, p. 292-308), Douglas (11), and Dusenberre (13). This method has the advantage of being simple and of being surprisingly accurate, but, as previously mentioned, has a severe limitation placed upon the size of the time increment.

For an infinite cylinder the heat Equation 5 can be written in a finite difference form. The first derivative term becomes, using  $x$  as the radial direction in place of  $r$ ,

$$\left. \frac{\partial T}{\partial x} \right|_m^n = \frac{T_{m+1}^n - T_{m-1}^n}{2\Delta x} + o(\Delta x^2) \quad (31)$$

and the second derivative becomes

$$\left. \frac{\partial^2 T}{\partial x^2} \right|_m^n = \frac{T_{m+1}^n - 2T_m^n + T_{m-1}^n}{\Delta x^2} + o(\Delta x^2). \quad (32)$$

Applying Equation 31 and 32 together with the fact that  $x = m\Delta x$  gives the right side of Equation 5 in difference form if  $m \neq 0$ ,

$$\begin{aligned} k \left( \frac{\partial^2 T}{\partial x^2} + \frac{1}{x} \frac{\partial T}{\partial x} \right) &= k \left[ \frac{T_{m+1}^n - 2T_m^n + T_{m-1}^n}{\Delta x^2} + \frac{1}{m\Delta x} \frac{T_m^{n+1} - T_m^{n-1}}{2\Delta x} \right] \\ &= \frac{k}{2m\Delta x^2} [(2m+1)T_{m+1}^n - 4mT_m^n + (2m-1)T_{m-1}^n] \quad (33) \end{aligned}$$

Using Equation 33 to replace the right side of Equation 5 and using Equation 29 to replace the left side of Equation 5 gives

$$\frac{T_m^{n+1} - T_m^n}{\Delta t} = \frac{k}{\rho C} \frac{1}{2m\Delta x^2} [(2m+1)T_{m+1}^n - 4mT_m^n + (2m-1)T_{m-1}^n] \quad (34)$$

Algebraic manipulation of Equation 34 gives

$$T_m^{n+1} = T_m^n + \frac{1}{M} \left[ \frac{2m+1}{2m} T_{m+1}^n - 2T_m^n + \frac{2m-1}{2m} T_{m-1}^n \right]. \quad (35)$$

For the special case of the center temperature of a cylinder if

$(dT/dx) = 0$  at  $x = 0$  (also  $m = 0$ ) the result (13, p. 67) is

$$T_0^{n+1} = T_0^n + \frac{4}{M} (T_1^n - T_0^n) . \quad (36)$$

Two other methods claimed by Larkin (27) to have stability superior to the ordinary explicit method, were evaluated for use in the present model. The increased stability would allow larger time increments and, thus, shorter computing time, and also it was claimed that the convergences of these methods were good. These methods were the Dufort and Frankel method (12) and an exponential method (27), and the specific equations for these methods are given in Appendix II.

A comparison of the accuracy of these two methods together with the conventional explicit method was based upon a solution of the temperature profile within an infinite cylinder being heated linearly at the surface. The heating rate was  $8 \frac{^{\circ}\text{C}}{\text{min}}$ , the radius of the cylinder was one centimeter, and the diffusivity of the material in the cylinder was  $0.006 \frac{\text{cm}^2}{\text{sec}}$ . The specific comparison is derived from the time required for the differential between the surface temperature and the center temperature to reach within 0.1% of the quasi-steady state temperature difference of  $5.5556^{\circ}\text{C}$  (found from Equation 8), for which an analytical solution applying Equation 6 gave an answer of 205.00 seconds. It was found that the exponential method did

not converge to the desired answer even for small increments so it was dropped from further consideration. The comparison of the accuracy and of the number of calculations between the Dufort and Frankel method and the ordinary explicit method are given in Table 1.

Several conclusions can be drawn from the figures in Table 1. (1) The conventional explicit method is stable for  $M = 2.5$ , which contradicts Dusenberre (13, p. 67) who claims a more severe criterion of  $M = 5.0$  for a cylinder. (2) The Dufort and Frankel method is about as accurate as the conventional explicit method during the cases when the latter method is stable. (3) The accuracy of the Dufort and Frankel method decreases when  $M = 1.25$ , where the other method is unstable. In conclusion, if an accuracy of  $\frac{1}{2}\%$  in this problem is desired, either of these methods is satisfactory, but if a larger error can be tolerated, the method of Dufort and Frankel can be considered superior due to its better stability. However, the conventional explicit method was chosen because of its greater simplicity.

In addition, the conventional explicit method was applied to a finite cylinder. It was found, however, that the extra calculations needed to determine the temperatures in two dimensions made the computer running time so long that the solution became too expensive monetarily. The equations that were used are given in Appendix IV.



Table 1. A comparison between the Durfort and Frankel Method (12) and the Conventional Explicit Method.

$M = \frac{\Delta x^2}{a\Delta t}$	$\Delta t$ sec	$\Delta x$ cm	Conventional Explicit Method			Duforth and Frankel Method		
			time	error	number of calculations	time	error	number of calculations
5.000	0.0833	0.05	205.083	+ .083	49,220	205.250	+0.250	49,260
2.500	0.1667	0.05	209.833	- .167	24,580	205.000	0	24,600
1.250	0.3333	0.05		unstable		203.667	-1.333	12,200
0.625	0.6667	0.05		unstable		198.000	-7.000	5,940
5.000	0.3333	0.10	205.333	+0.333	6,160	206.000	+1.000	6,180
2.500	0.6667	0.10	204.000	-1.000	3,060	204.667	-0.333	3,070
1.250	1.3333	0.10		unstable		198.667	-6.333	1,490
5.000	1.3333	0.20	205.333	+0.333	770	208.000	+3.000	780
2.500	2.6667	0.20	200.000	-5.000	375	202.667	-2.333	380
1.250	5.3333	0.20	---	---	---	176.000	-29.000	165

### The Boundary Equations

In addition to the finite difference Equations 35 and 36, equations for the temperatures near the boundary which are applicable to unevenly spaced distance intervals, and equations for the movement of the boundary were required. These equations were derived in two different finite difference forms: three-point formulas derived from Lagange's interpolation formula 17, and two-point formulas derived from a central difference formula similar to Equation 30. After derivation, the better of these two types of boundary equations was chosen on the basis of the convergence of the final solutions.

These boundary equations were derived by considering the arrangement shown in Figure 5, which depicts a unit length of one half of an axial cross section through the center of an infinite cylinder. Consider that this cylinder is divided into  $K$  annular shells of thickness  $\Delta x$ , and that the lines bounding the shells are located at distances  $0, \Delta x, 2\Delta x, \dots, m\Delta x, \dots, (K-1)\Delta x$ , and  $K\Delta x$  from the center. The location of the phase boundary at the transition temperature,  $T_L$ , is a distance,  $x(n\Delta t)$ , from the center, and this distance is also specified relative to a nearby divisional line by the ratio,  $p$  ( $1 < p \leq 2$ ). The necessary equations must give the temperatures at points  $m + 1$  and  $m - 2$ , and account for the boundary movement. The calculation of temperatures at point  $m$  or at point  $m - 1$  was

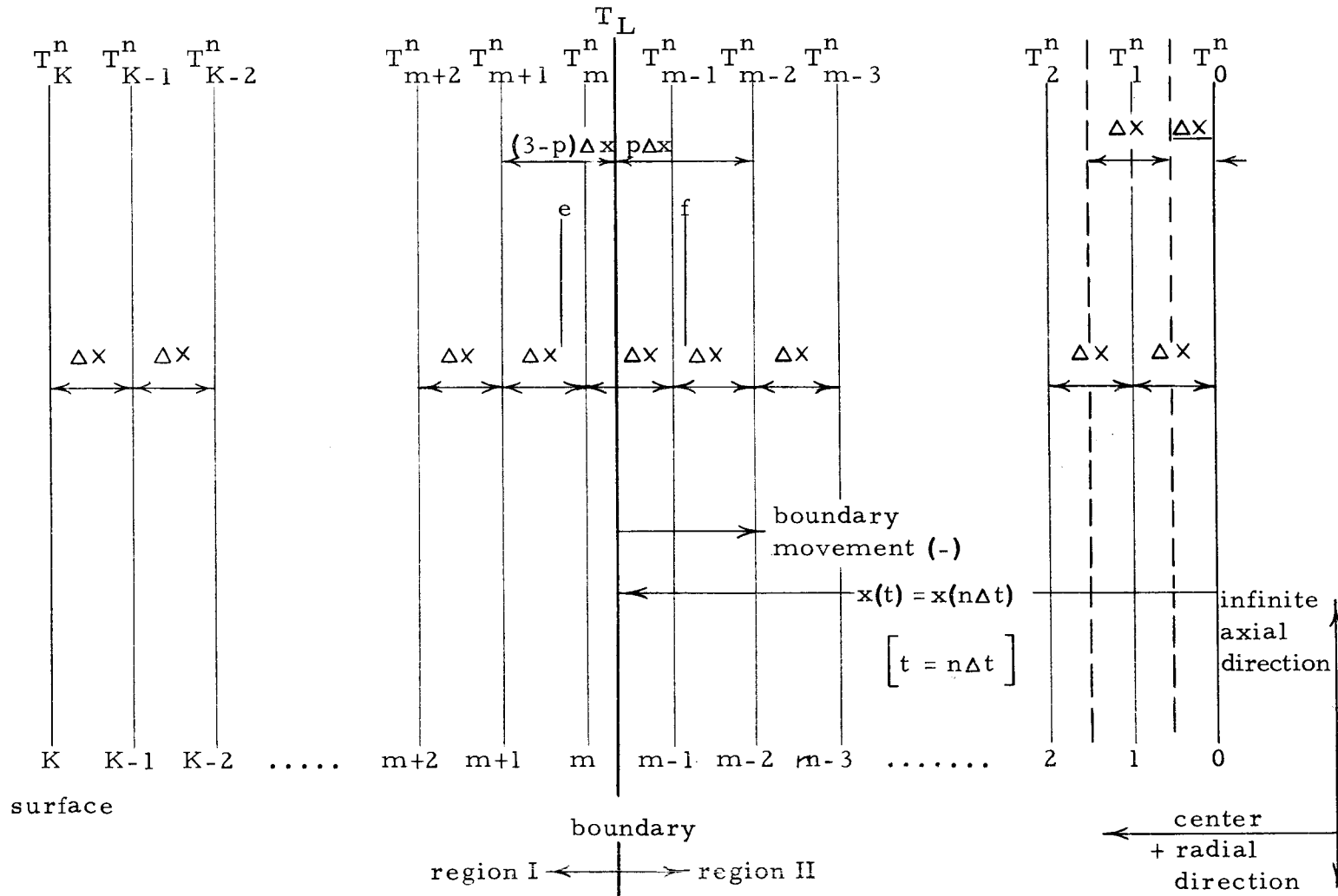


Figure 5. Diagram showing the division of the infinite-cylindrical sample into cylindrical shells.

deferred until the boundary had moved at least a distance of  $\Delta x$  away from the respective point because an instability occurred in the solution when  $p$  was smaller than one, or larger than two.<sup>6/</sup>

### Three-point Equations

The three-point equations which were used to calculate  $T_{m+1}^n$  and  $T_{m-2}^n$  were derived using Equation 20 and 29 substituted into the heat Equation 5. When these substitutions are made, the result is

$$\begin{aligned} \frac{T_m^{n+1} - T_m^n}{\Delta t} = 2 \left[ \frac{T(a_0)}{(a_0 - a_1)(a_0 - a_2)} + \frac{T(a_1)}{(a_1 - a_0)(a_1 - a_2)} + \frac{T(a_2)}{(a_2 - a_0)(a_2 - a_1)} \right] \\ + \frac{1}{x} \left[ \frac{(x - a_1) + (x - a_2)}{(a_0 - a_1)(a_0 - a_2)} T(a_0) + \frac{(x - a_0) + (x - a_2)}{(a_1 - a_0)(a_1 - a_2)} T(a_1) \right. \\ \left. + \frac{(x - a_0) + (x - a_1)}{(a_2 - a_0)(a_2 - a_1)} T(a_2) \right]. \end{aligned} \quad (37)$$

When finding  $T_{m+1}^n$ , definitions can be made, referring to Figure 5, that

---

<sup>6</sup>This instability can be explained by noting that the condition for stability in an equation for  $T_{m-2}^n$ ,  $M = \frac{p\Delta x^2}{\alpha \Delta t} \geq 5$ , is violated for  $p < 1$  if the increments have been chosen so that  $M = 5$  when  $p = 1$ . An analogous treatment shows that an instability results in the equation for  $T_m^n + 1$  when  $p > 2$ .

$$\begin{aligned}
a_0 &= (m+2)\Delta x \\
a_1 &= (m+1)\Delta x \\
a_2 &= x(t) \\
x(t) &= (m-2+p)\Delta x \\
x &= a_1 .
\end{aligned} \tag{38}$$

Substitution of Equation 38 into 37 and rearranging gives

$$\begin{aligned}
T_{m+1}^{n+1} &= T_{m+1}^n + \frac{1}{M} \left\{ \frac{(3-p)(m+2)}{(4-p)(m+1)} \left[ \frac{5-p}{4-p} T_{m+2}^n + \frac{4-p}{p-3} T_{m+1}^n + \frac{1}{(p-3)(p-4)} T_L \right] \right. \\
&\quad + \frac{2-p}{p-3} \left[ \frac{3-p}{4-p} T_{m+2}^n + \frac{p-2}{3-p} T_{m+1}^n + \frac{1}{(p-4)(3-p)} T_L \right] \\
&\quad \left. + \frac{m-2+p}{(p-3)(4-p)(m+1)} \left[ \frac{p-3}{4-p} T_{m+2}^n + \frac{4-p}{3-p} T_{m+1}^n + \frac{2p-7}{(p-4)(p-3)} T_L \right] \right\}
\end{aligned} \tag{39}$$

Similarly, in finding  $T_{m-2}^n$ , it can be defined that

$$\begin{aligned}
a_0 &= x(t) \\
a_1 &= (m-2)\Delta x \\
a_2 &= (m-3)\Delta x \\
x(t) &= (m-2+p)\Delta x \\
x &= a_1 .
\end{aligned} \tag{40}$$

Then Equations 40 and 37 are used to give

$$\begin{aligned}
T_{m-2}^{n+1} = T_{m-2}^n + \frac{1}{M} & \left\{ \frac{(m-2+p)}{(m-2)p(p+1)} \left[ \frac{2p+1}{p(p+1)} T_L - \frac{p+1}{p} T_{m-2}^n + \frac{p}{p+1} T_{m-3}^n \right] \right. \\
& + \frac{p-1}{p} \left[ \frac{1}{p(p+1)} T_L + \frac{p-1}{p} T_{m-2}^n - \frac{p}{p+1} T_{m-3}^n \right] - \frac{p(m-3)}{(p+1)(m-2)} \\
& \left. \left[ \frac{-1}{p(p+1)} T_L + \frac{p+1}{p} T_{m-2}^n - \frac{p+2}{p+1} T_{m-3}^n \right] \right\}. \quad (41)
\end{aligned}$$

The equations for the boundary movement can be derived by using Equation 18. After applying Equation 38 to 18 in region I of Figure 5, the gradient at the boundary can be written as

$$\frac{dT}{dx} \Big|_I^n \cong \frac{p-3}{(4-p)\Delta x} T_{m+2}^n + \frac{p-4}{(p-3)\Delta x} T_{m+1}^n + \frac{2p-7}{\Delta x(p-3)(p-4)} T_L. \quad (42)$$

Similarly, after applying Equation 40 to 18 in region II, the gradient at the boundary can be written as

$$\frac{dT}{dx} \Big|_{II}^n \cong \frac{2p+1}{p(p+1)\Delta x} T_L - \frac{p+1}{p\Delta x} T_{m-2}^n + \frac{p}{(p+1)\Delta x} T_{m-3}^n. \quad (43)$$

Thus since  $A_b = A_1 = A_2$  (because Equation 42 and 43 give the gradient exactly on the boundary) substituting Equation 42 and 43 into 28 gives the final result as

$$\begin{aligned}
\delta x = \frac{\Delta t}{\rho \Delta H} & \left\{ \frac{k_I}{\Delta x} \left[ \frac{p-3}{4-p} T_{m+2}^n + \frac{p-4}{p-3} T_{m+1}^n + \frac{2p-7}{(p-3)(p-4)} T_L \right] \right. \\
& \left. + \frac{k_{II}}{\Delta x} \left[ \frac{2p+1}{p(p+1)} T_L - \frac{p+1}{p} T_{m-2}^n + \frac{p}{p+1} T_{m-3}^n \right] \right\}. \quad (44)
\end{aligned}$$

### Two-point Equations

The two-point equations offer an alternate formulation for the boundary equations. The first distance derivative of temperature at a point between sections can be approximated by using temperatures at the midpoints of the two contingent sections and by using the distance between these midpoint temperatures as

$$\left. \frac{dT}{dx} \right|_m^n \approx \frac{T_{m+\frac{1}{2}}^n - T_{m-\frac{1}{2}}^n}{\Delta x} \quad (45)$$

For the unequally sized segments of Figure 5 a new form evolves as

$$\left. \frac{dT}{dx} \right|_{m+1}^n \approx \frac{T_{m+1+\frac{1}{2}}^n - T_e^n}{\frac{\Delta x}{2} + \frac{(3-p)\Delta x}{2}} \quad (46)$$

where  $e$  denotes a position of  $T_e^n$  at  $(m-\frac{1}{2}+\frac{p}{2})\Delta x$ .

The second derivative at point  $m+1$  is obtained by writing the derivative of Equation 46 as

$$\frac{d}{dx} \left( \frac{dT}{dx} \right) \Big|_{m+1}^n \approx \frac{\left. \frac{dT}{dx} \right|_{m+1+\frac{1}{2}}^n - \left. \frac{dT}{dx} \right|_e^n}{\frac{\Delta x}{2} + \frac{(3-p)\Delta x}{2}} \quad (47)$$

The term  $\left. \frac{dT}{dx} \right|_{m+1+\frac{1}{2}}^n$  is easily found from Equation 45 as

$$\left. \frac{dT}{dx} \right|_{m+1}^n \cong \frac{T_{m+2}^n - T_{m+1}^n}{\Delta x} . \quad (48)$$

$\left. \frac{dT}{dx} \right|_e^n$  is slightly more complex. The result from Equation 45 is

$$\left. \frac{dT}{dx} \right|_e^n \cong \frac{T_{m+1}^n - T_L}{(3-p)\Delta x} . \quad (49)$$

Substitution of Equation 48 and 49 into 47 gives, after algebraic manipulation,

$$\left. \frac{d^2T}{dx^2} \right|_{m+1}^n \cong \left( \frac{2}{\Delta x^2} \right) \frac{(3-p)T_{m+2}^n + (p-4)T_{m+1}^n + T_L}{(3-p)(4-p)} . \quad (50)$$

The first derivative of  $T_{m+1}^n$  can be written as

$$\left. \frac{dT}{dx} \right|_{m+1}^n \cong \frac{T_{m+2}^n - T_L}{(4-p)\Delta x} . \quad (51)$$

Using Equation 50 and 51, the right side of the heat Equation 5 becomes

$$\left( \frac{1}{x} \frac{dT}{dx} + \frac{d^2T}{dx^2} \right) \Big|_m^n \cong \frac{1}{x} \left[ \frac{T_{m+2}^n - T_L}{(4-p)\Delta x} \right] + 2 \frac{(3-p)T_{m+2}^n + (p-4)T_{m+1}^n + T_L}{(3-p)(4-p)\Delta x^2} . \quad (52)$$

Finally, after applying Equation 52 and 29, the heat equation in finite difference form can be written as



$$\frac{T_{m+1}^{n+1} - T_{m+1}^n}{\Delta t} = \frac{k}{\rho C} \frac{1}{\Delta x} \left[ \frac{T_{m+2}^n - T_L}{(x)(4-p)} + 2 \frac{(3-p)T_{m+2}^n + (p-4)T_{m+1}^n + T_L}{(3-p)(4-p)\Delta x} \right] \quad (53)$$

Thus, the temperature at  $x = (m+1)\Delta x$  can be found, after some algebraic manipulation of Equation 53, from

$$T_{m+1}^{n+1} = T_{m+1}^n + \frac{1}{M} \left\{ \frac{[x+(3-p)\Delta x][T_{m+2}^n - T_{m+1}^n] - [\frac{x}{3-p} + \frac{\Delta x}{2}][T_{m+1}^n - T_L]}{(4-p)x + \frac{\Delta x}{4} (3p^2 - 22p + 40)} \right\} \quad (54)$$

In an analogous derivation  $T_{m-2}^n$  was found to be

$$T_{m-2}^{n+1} = T_{m-2}^n + \frac{1}{M} \left\{ \frac{[\frac{x}{p} - \frac{\Delta x}{2}][T_L - T_{m-2}^n] - [x - (p+\frac{1}{2})\Delta x][T_{m-2}^n - T_{m-3}^n]}{(p+1)x - \frac{\Delta x}{4} (3p^2 + 4p + 1)} \right\} \quad (55)$$

The two-point equation for the boundary movement must now be considered. The derivative at the boundary in region II may be written as

$$\left. \frac{dT}{dx} \right|_f^n \cong \frac{T_L - T_{m-2}^n}{p\Delta x} \quad (56)$$

where  $f$  signifies the location  $x = (m-2+p/2)\Delta x$ . Also, the following areas may be calculated (because the two-point equations for the gradients are considered at  $e$  and  $f$  rather than exactly at the boundary):

$$A_f = \pi[x(t) - p\Delta x/2] \quad (57a)$$

$$A_b = \pi x(t) \quad (57b)$$

$$A_e = \pi[x(t) + (3-p)\Delta x/2] . \quad (57c)$$

These areas plus Equations 49 and 56 were substituted into 38 to give

$$\delta x = \frac{\Delta t}{x(t)\rho\Delta H} \left\{ -\frac{k_1}{\Delta x} [x(t) + (3-p)\Delta x/2] \left[ \frac{T_{m+1}^n - T_L}{3-p} \right] + \frac{k_2}{\Delta x} [x(t) - p\Delta x/2] \left[ \frac{T_L - T_{m-2}^n}{p} \right] \right\}. \quad (58)$$

### Special Cases

When the boundary is close to grid points near the extremities of the grid, the previously derived equations do not apply, so special equations were needed. Only an outline of the reasoning leading to these equations will be offered here.

The equation for  $T_0^n$ , when the boundary is near the center, is simply

$$T_0^n = T_L . \quad (59)$$

This equation is valid if it can be assumed (and this assumption was later supported by the solution of model) that by the time the boundary has approached close to the center, the temperature at the center has already asymptotically reached the transition temperature. Also, it directly follows from Equation 59 that when the boundary is near to

the center there is a zero temperature gradient inside the boundary in region II, and the Equation 28 can be simplified to

$$\delta x = - \frac{k_1 A_1 \Delta t}{A_b \rho \Delta H} \left. \frac{dT}{dx} \right|_1 . \quad (60)$$

When the two-point Equation 49 for the gradient in region I and the areas from Equation 57b and 57c are substituted into Equation 60, the result is

$$\delta x = -k_1 \Delta t \frac{x(t) + (3-p)\Delta x/2}{x(t)\rho\Delta H(3-p)\Delta x} (T_{m+1}^n - T_L) . \quad (61)$$

When the three-point Equation 42 is used (since in this case  $A_1 = A_b$ ), the result is

$$\delta x = \frac{-k_1 \Delta t}{\Delta x \rho \Delta H} \left[ \frac{p-3}{(4-p)} T_{m+2}^n + \frac{p-4}{p-3} T_{m+1}^n + \frac{2p-7}{(p-3)(p-4)} T_L \right] . \quad (62)$$

A rather complex equation for  $\delta x$  is necessary near the beginning of the phase change when the boundary is in the outermost two sections. The gradient in region I can be written as

$$\left. \frac{dT}{dx} \right|_1 = \frac{T_K^n - T_L}{K \Delta x - x(t) - \delta x/2} . \quad (63)$$

Substituting Equation 63 into 28 gives the equation implicit in  $\delta x$ ,

$$\delta x = \frac{\Delta t}{\rho \Delta H} - k_1 \frac{T_K^n - T_L}{K \Delta x - x(t) - \delta x / 2} + k_2 \left. \frac{dT}{dx} \right|_2 . \quad (64)$$

To solve for  $\delta x$ , a specific expression for  $\left. \frac{dT}{dx} \right|_2$  is substituted into Equation 64, and the resulting equation is solved using the quadratic equation (18, p. 318). For example, substituting the two-point formula (Equation 56) for  $\left. \frac{dT}{dx} \right|_2$  into Equation 64 and solving for  $\delta x$  gives

$$\delta x = K \Delta x - x(t) + \frac{\Delta t k_2 (T_L - T_{m-2}^n)}{2 \rho \Delta H p \Delta x} - \left\{ \left[ x(t) - K \Delta x - \frac{\Delta t k_2 (T_L - T_{m-2}^n)}{2 \rho \Delta H \Delta x p} \right]^2 - \frac{2 \Delta t}{\rho \Delta H} \left[ \frac{k_2 (T_L - T_{m-2}^n) (K \Delta x - x(t))}{p \Delta x} - k_1 \phi \left( \ell - \frac{1}{2} \right) \Delta t \right] \right\}^{\frac{1}{2}} \quad (65)$$

for the  $K$ th section, where  $\ell$  designates the  $\ell$ th time increment,  $\Delta t$ , since the phase change began. The negative of the square root term was used because a plus sign would give a positive  $\delta x$ , which is untenable with physical reality, since the boundary is moving inward in a negative radial direction. The analogous result for the three-point equation is

$$\begin{aligned}
\delta x = & \frac{\Delta t k_2}{2\rho\Delta H\Delta x} \left[ \frac{2p+1}{p(p+1)} T_L - \frac{p+1}{p} T_{K-2}^n + \frac{p}{p+1} T_{K-3}^n \right] - x(n\Delta t) + K\Delta x \\
& - \left\{ \left[ \frac{\Delta t k_2}{2\rho\Delta H\Delta x} \left( \frac{2p+1}{p(p+1)} T_L - \frac{p+1}{p} T_{K-2}^n + \frac{p}{p+1} T_{K-3}^n \right) - x(n\Delta t) + K\Delta x \right]^2 \right. \\
& + \frac{2\Delta t k_2}{\rho\Delta H\Delta x} \left( \frac{2p+1}{p(p+1)} T_L - \frac{p+1}{p} T_{K-2}^n + \frac{p}{p+1} T_{K-3}^n \right) (x(n\Delta t) - K\Delta x) \\
& \left. + \frac{\bar{\Delta t}^2 k_1 \phi}{\rho\Delta H x(n\Delta t)} (K\Delta x + x(n\Delta t)) \left( \ell - \frac{1}{2} \right) \right\}^{\frac{1}{2}}. \tag{66}
\end{aligned}$$

In the  $(K-1)^{\text{th}}$  section, Equation 64 can be simplified, because the term  $\delta x/2$  is generally much smaller than  $K\Delta x - x(t)$ . When this  $\delta x/2$  term is dropped, the quadratic formula is not needed since Equation 64 becomes explicit in  $\delta x$ . The result for the two-point equation is

$$\delta x = - \frac{\Delta t}{\rho\Delta H\Delta x x(n\Delta t)} \left[ \frac{k_1 \phi(\ell)\Delta t}{2(3-p)} (K\Delta x + x(n\Delta t)) - k_2 (T_L - T_{K-3}^n) \left( \frac{x(n\Delta t)}{p} - \frac{\Delta x}{2} \right) \right], \tag{67}$$

and the result for the three-point equation is

$$\delta x = \frac{\Delta t}{\rho\Delta H} \left[ - \frac{k_1 \phi \ell \Delta t}{K\Delta x - x(n\Delta t)} + \frac{k_2}{\Delta x} \left( \frac{2p+1}{p(p+1)} T_L - \frac{p+1}{p} T_{K-3}^n + \frac{p}{p+1} T_{K-4}^n \right) \right]. \tag{68}$$

As was mentioned before, the temperature  $T_m^n$  is not calculated when the boundary lies between grid lines  $m$  and  $m-1$ , but when the boundary has just moved past  $m-1$ ,  $T_m^n$  must be calculated. The usual Langrange's three-point interpolation formula

(Equation 17) was used for this calculation during the time increment just after the boundary has crossed the line  $m-1$ . This equation can be written

$$T_m^n = \frac{p-3}{5-p} T_{m+2}^n + \frac{2(p-3)}{p-4} T_{m+1}^n + \frac{2}{(p-5)(p-4)} T_L \cdot \quad (69)$$

The only remaining equation which was needed describes the temperature at the surface of the cylinder. This equation is

$$T_K^n = \phi n \Delta t + T_K^0 \quad (70)$$

where  $\phi$  is the heating rate in  $^{\circ}\text{C}/\text{sec}$ , and  $n$  designates the  $n^{\text{th}}$  time increment,  $\Delta t$ , since the heating began from an initial surface temperature of  $T_K^0$ . These finite difference equations for the model were then solved by employing a digital computer.

### The Digital Computer Solution

The programs for use on a digital computer, written in FORTRAN IV computer language (8, 32), for the cases of the three-point and two-point boundary equations are given in Appendix III. In addition, a schematic block diagram of the program is given in Appendix III.

The numerical solution was performed on a Control Data Corporation Model 3300 computer located at the Oregon State University

Computer Center. This machine has a facility which will plot the output graphically, and this facility was used to give many of the theoretical DTA peaks directly in graphical form.

Preliminary results of the numerical solution of the model were used to choose between the two-point and three-point boundary equations based upon the convergences of the final solutions. The data of Tsang (45) for the infinite cylinder with a heating rate of  $30^{\circ}\text{C}/\text{min}$  was used in these solutions. The effect of changing the number of segments used in the solution is shown in Figure 6, and this is an indication of convergence. It is clear from Figure 6 that the two-point equations have converged to a solution at a division of ten segments, but the three-point equations still haven't shown convergence at twenty segments. Also, it can be seen from the extrapolation of this curve for the three-point equations that the solution of the three-point equations would probably converge to the same solution as the two-point equations if additional segments would be used. Furthermore, the three-point equations are more complicated than the two-point equations, and as a result, computer time used by a solution employing the three-point equations is significantly larger than the computer time used by a corresponding solution employing the two-point equations. Therefore, because of the better convergence and shorter running time for the two-point equations, these equations were chosen for the final model.

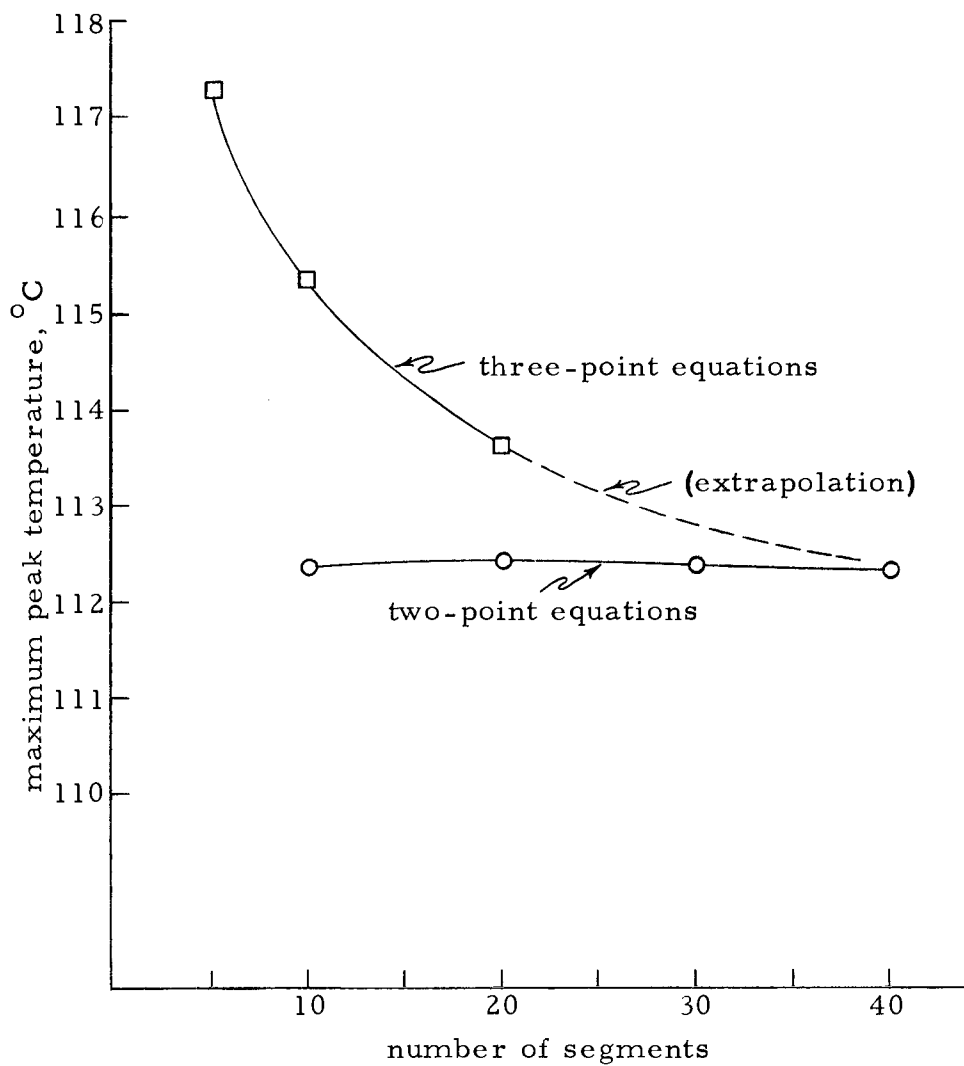


Figure 6. Convergence of the present model for two types of difference equations.



## RESULTS AND DISCUSSION

Results were calculated by a digital computer (CDC 3300) for the mathematical formulations developed. The computer not only gave printed answers but also graphically plotted the theoretical peaks. These peaks were the final tangible product of this study to be validated by comparison with previous work, both theoretical and experimental.

### Comparison with Previous Results

The present model, using the data and the physical assumptions of Tsang (45), produced a peak which is shown with two peaks of Tsang in Figure 7. Since the present model divided the infinite cylinder into twenty sections against one section and two sections for Tsang, the present method should be more accurate, although the meaning of a segment in each method is not exactly the same. The trend of using additional segments in Tsang's method, shown in Figure 7, is an increase in the maximum peak temperature, and it is highly possible that the results of the present model and Tsang's model would have been the same if Tsang's method had used several more segments.

When the present model employed the data of the DTA system described earlier, the result was the theoretical DTA curves for

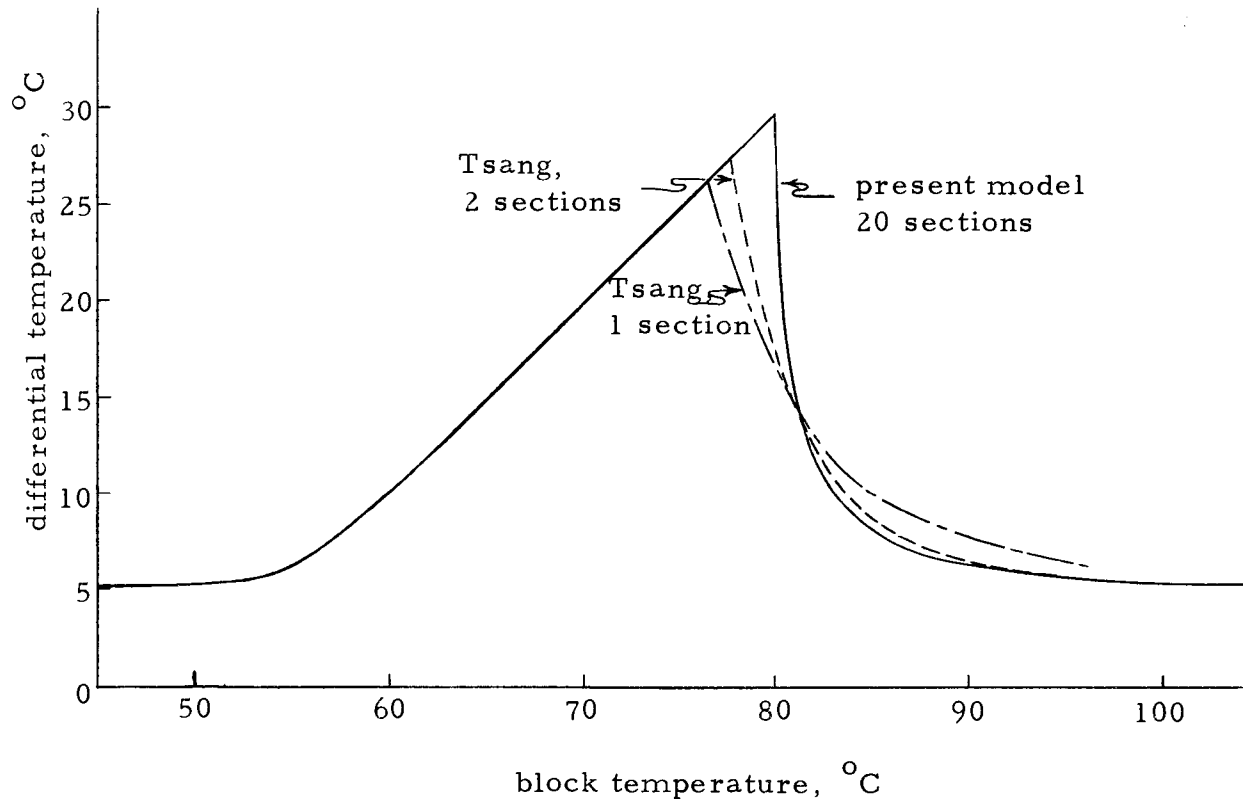


Figure 7. Comparison between the peaks of the present model and the peaks of Tsang (45).

quartz shown in Figure 8 and Figure 9 for four different heating rates. These peaks show the same variations with heating rates as previous experimental results have shown (1, 3) and two of these variations are shown in Figure 10: that of the peak area, and in Figure 11: that of maximum peak temperature. The present model and past experiments both show that the peak area increases linearly with temperature (3) and that the maximum peak temperature increases with temperature (1, 3). However, the theoretical results show a concave downward slope of the maximum peak temperature versus heating rate curve while experimental results give a concave upward slope, and this discrepancy has not been explained.

In addition the peaks in Figure 8 and Figure 9 look qualitatively like experimental peaks shown in Figure 12a for Berkelhamer (4) and Figure 12b for Keith and Tuttle (21). Berkelhamer's peak, which was run at a heating rate of 10 or 11 degrees per minute, shows more curvature than those of the present model, but much of this may be accounted for in error in the value for thermal conductivity. Keith and Tuttle's peak, run at a very slow heating rate of about  $0.6^{\circ}\text{C}$  per minute, also looks much like those of the present model, the major discrepancy being in the roundness of the top of the peak. But this roundness was probably due to a thermocouple being off center or due to a sample being inhomogeneous so that the phase boundary would not have reached the center thermocouple from all sides at

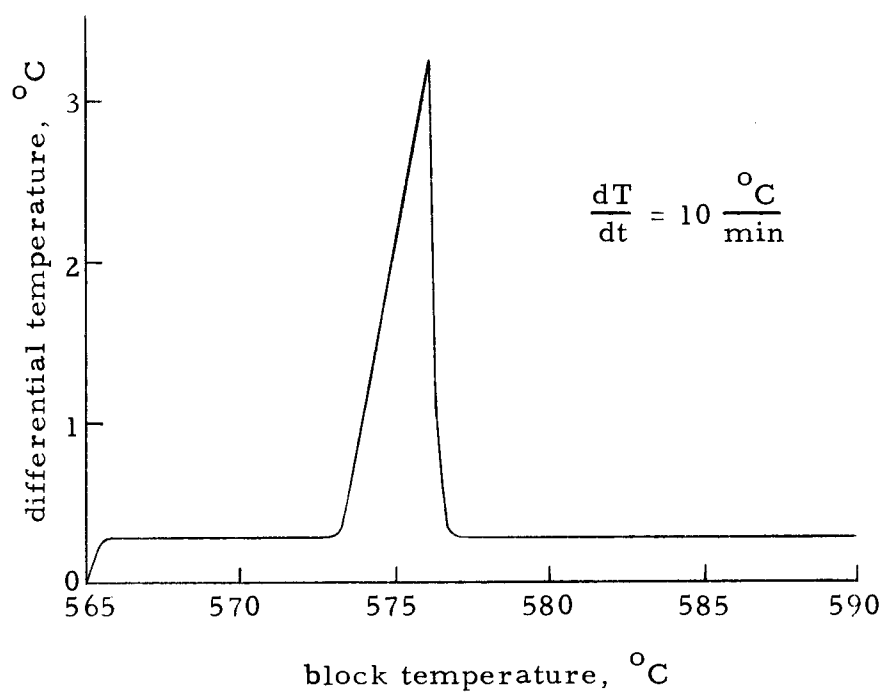
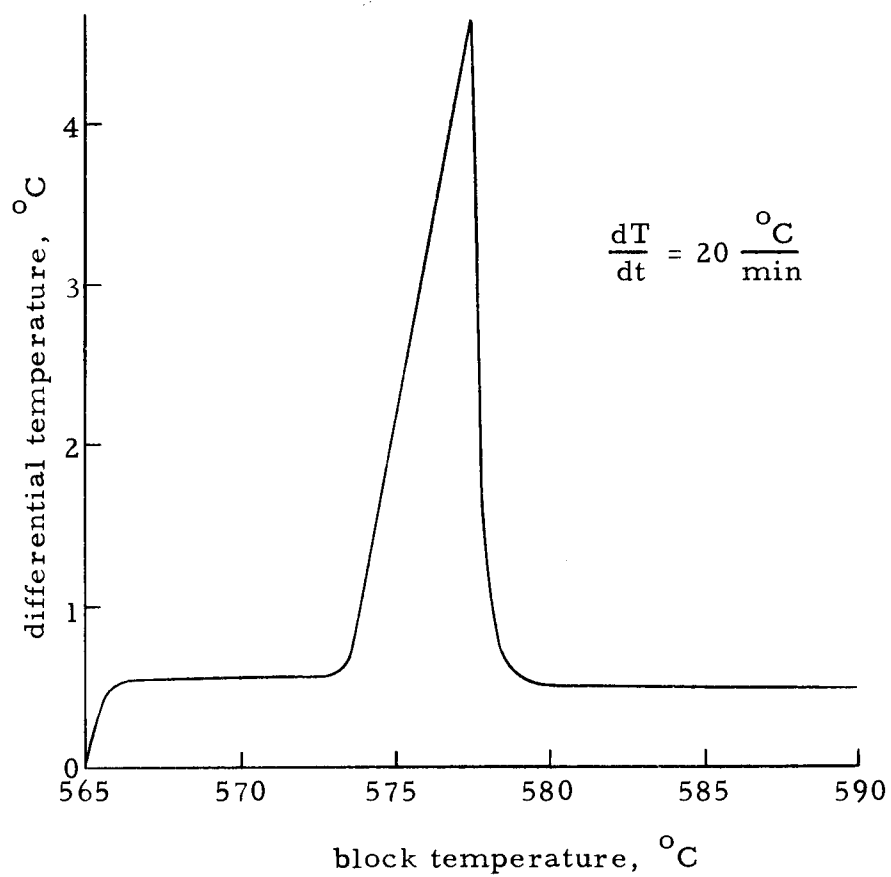


Figure 8. Theoretical DTA peaks of the present model for quartz.

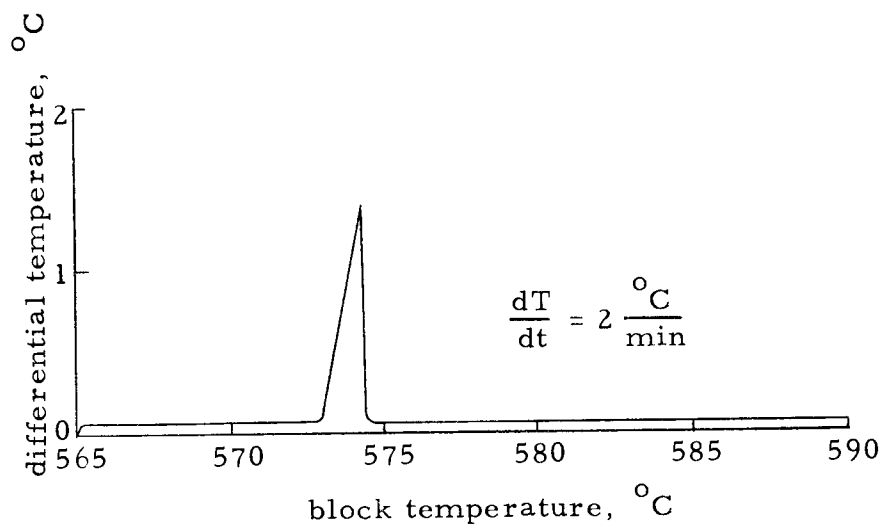
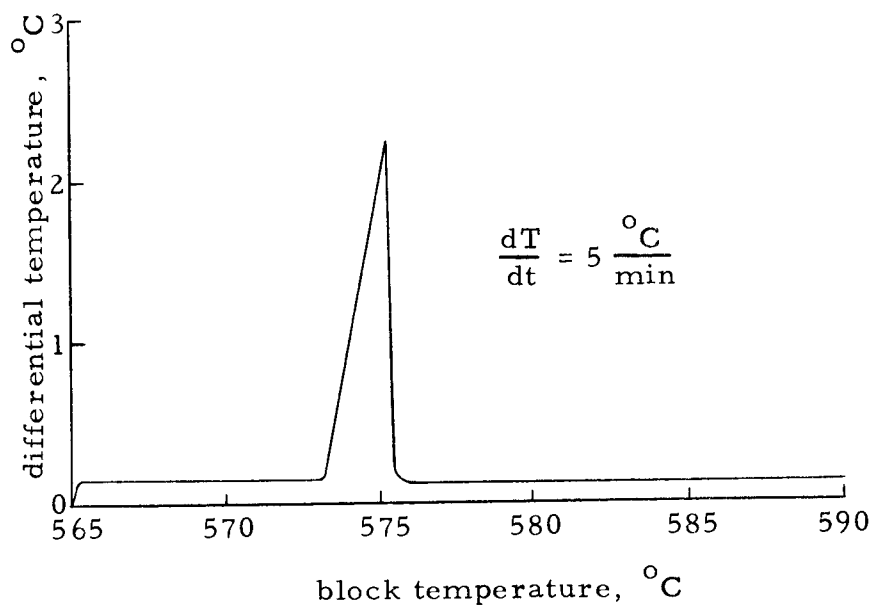


Figure 9. Theoretical DTA peaks of the present model for quartz.

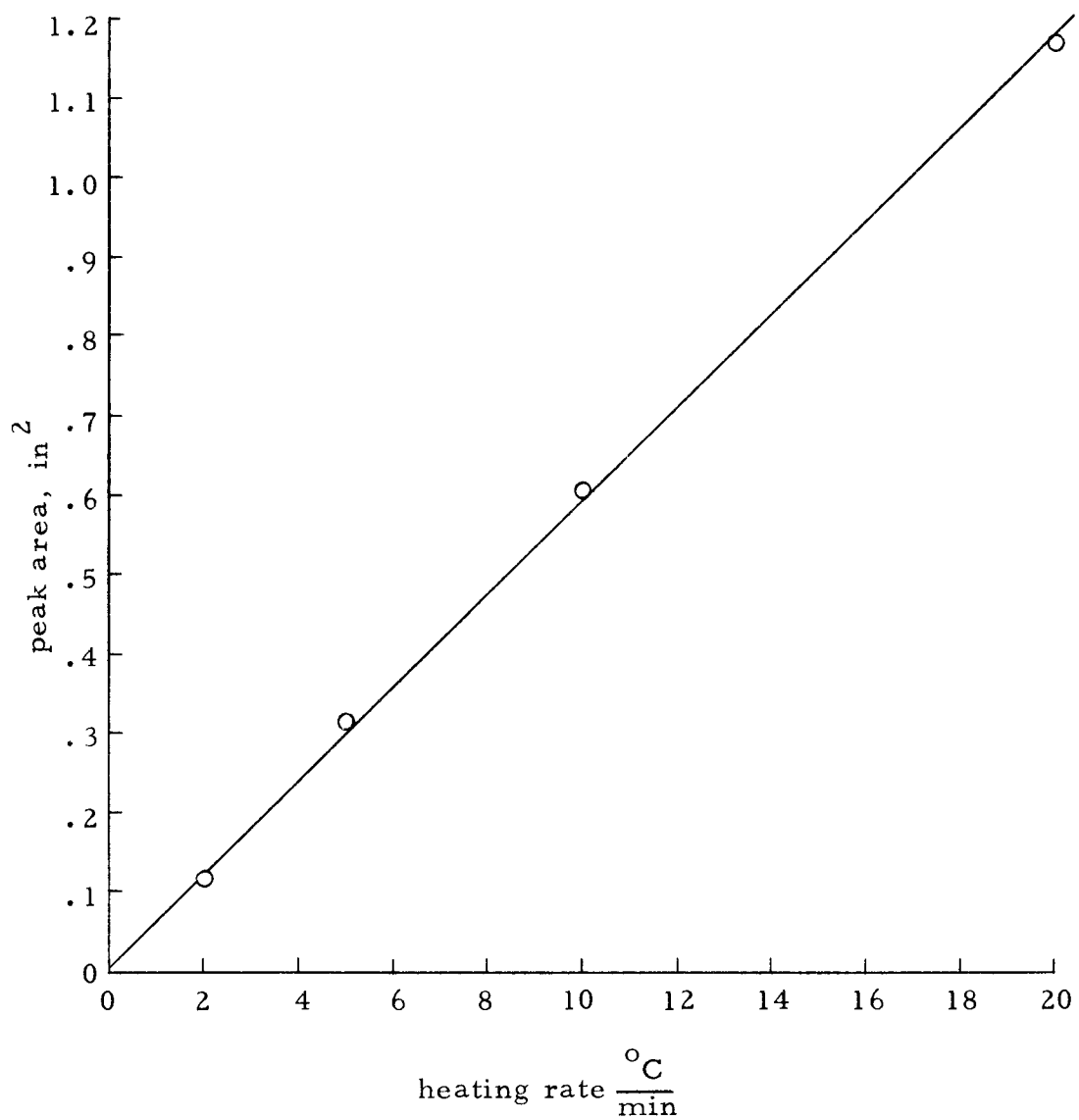


Figure 10. Effect of heating rate upon peak area.

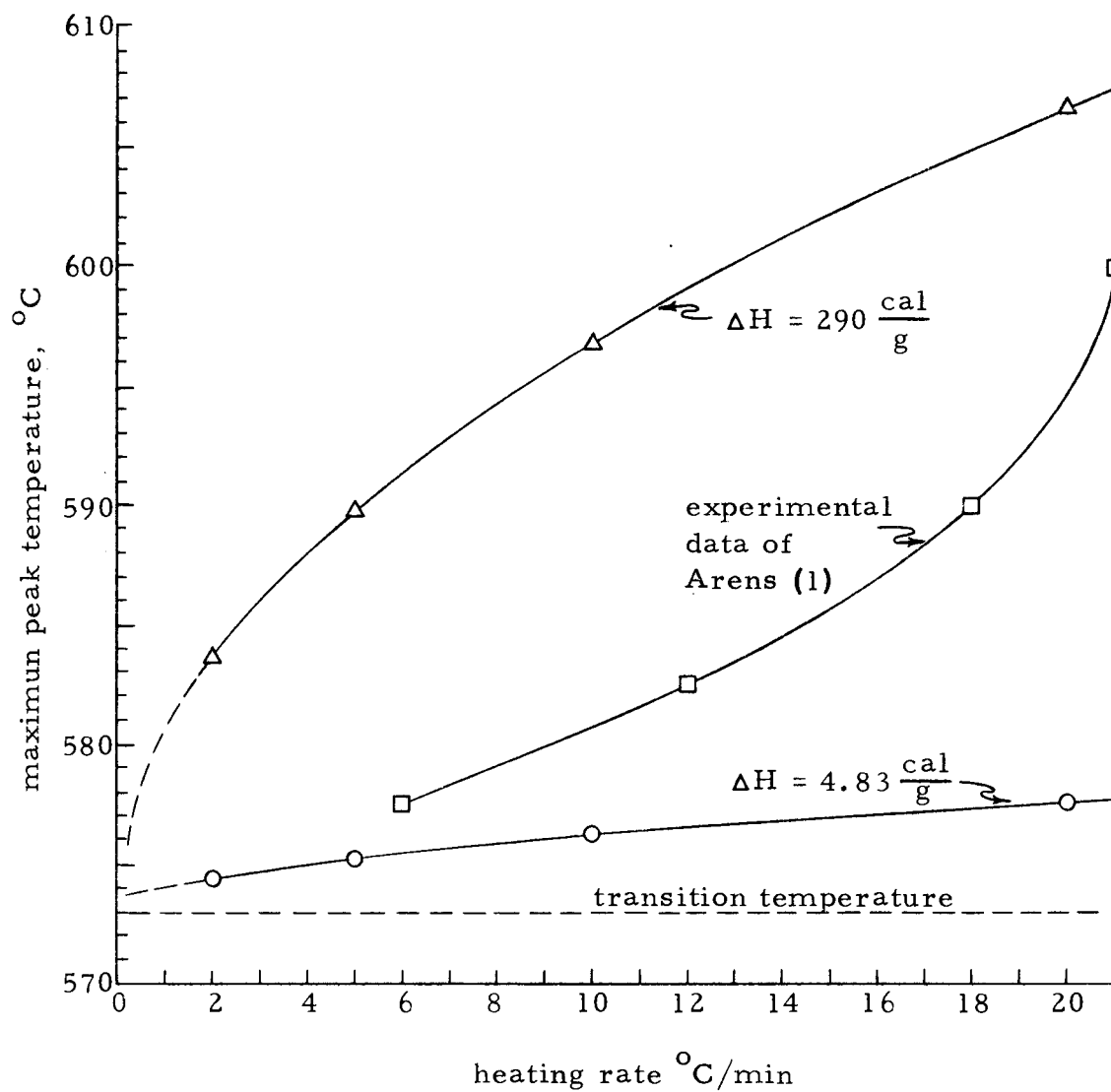


Figure 11. Effect of heating rate upon maximum peak temperature.

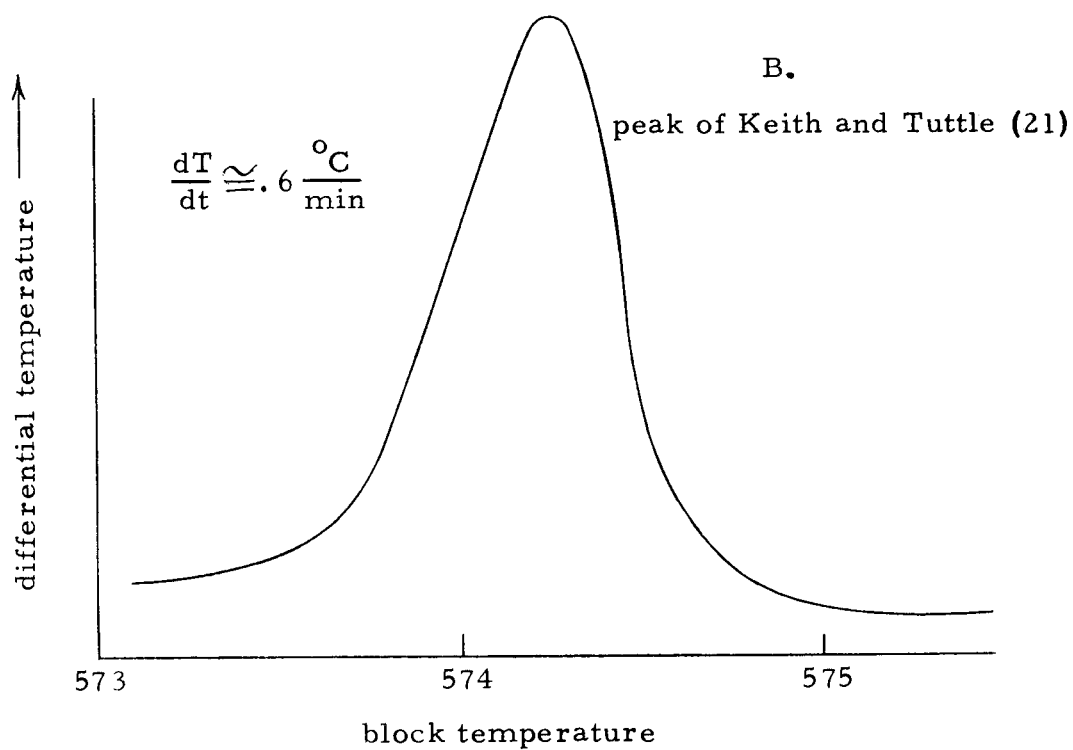
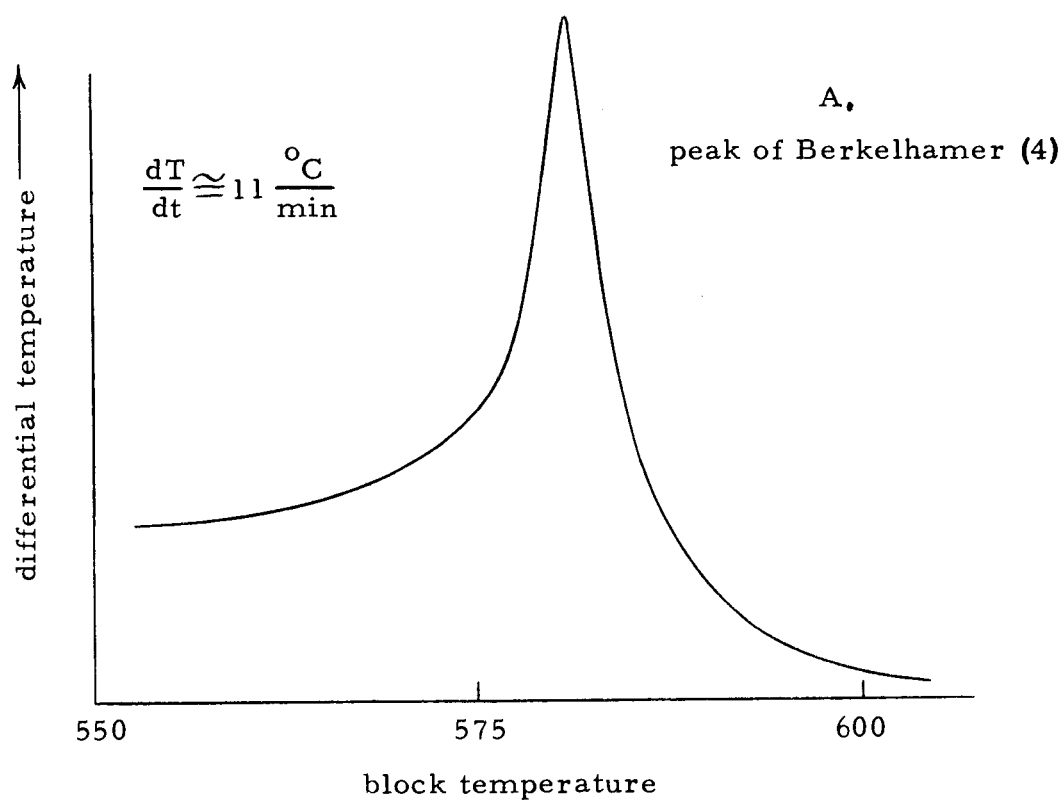


Figure 12. Experimental DTA peaks for quartz.



the same instant (38). While the conditions of these experiments were not identical with those of the present model, it was concluded that the qualitative comparisons are reasonably close.

Unfortunately, in most experimental peaks, like those in Figure 12, the actual value of  $\Delta T$  is not given, but instead, only deflections on the thermogram proportional to  $\Delta T$ . As a result, a quantitative comparison of  $\Delta T$  between theoretical results and experimental results is not possible, and only a qualitative comparison can be made. Specifically, this means that at present the qualitative shapes of the curves are the chief indicators of the validity of the theoretical model in predicting experimental peaks. Certainly this lack of experimental magnitudes for  $\Delta T$  is a void which needs to be filled before a real quantitative model is possible.

#### Sample Properties and Peak Shape

As one would expect the shape of the peak is determined largely by the thermal properties used in a test sample of the theoretical model. This difference is exemplified by the two peaks in Figure 13. One peak in Figure 13a, shaped like a right triangle, was produced using a heat of reaction approximately 60 times larger than was used by the other peak of Figure 13a. One peak in Figure 13b, which has curvature more like experimental peaks than the other peaks generated theoretically, used a heat of reaction of the same value but a

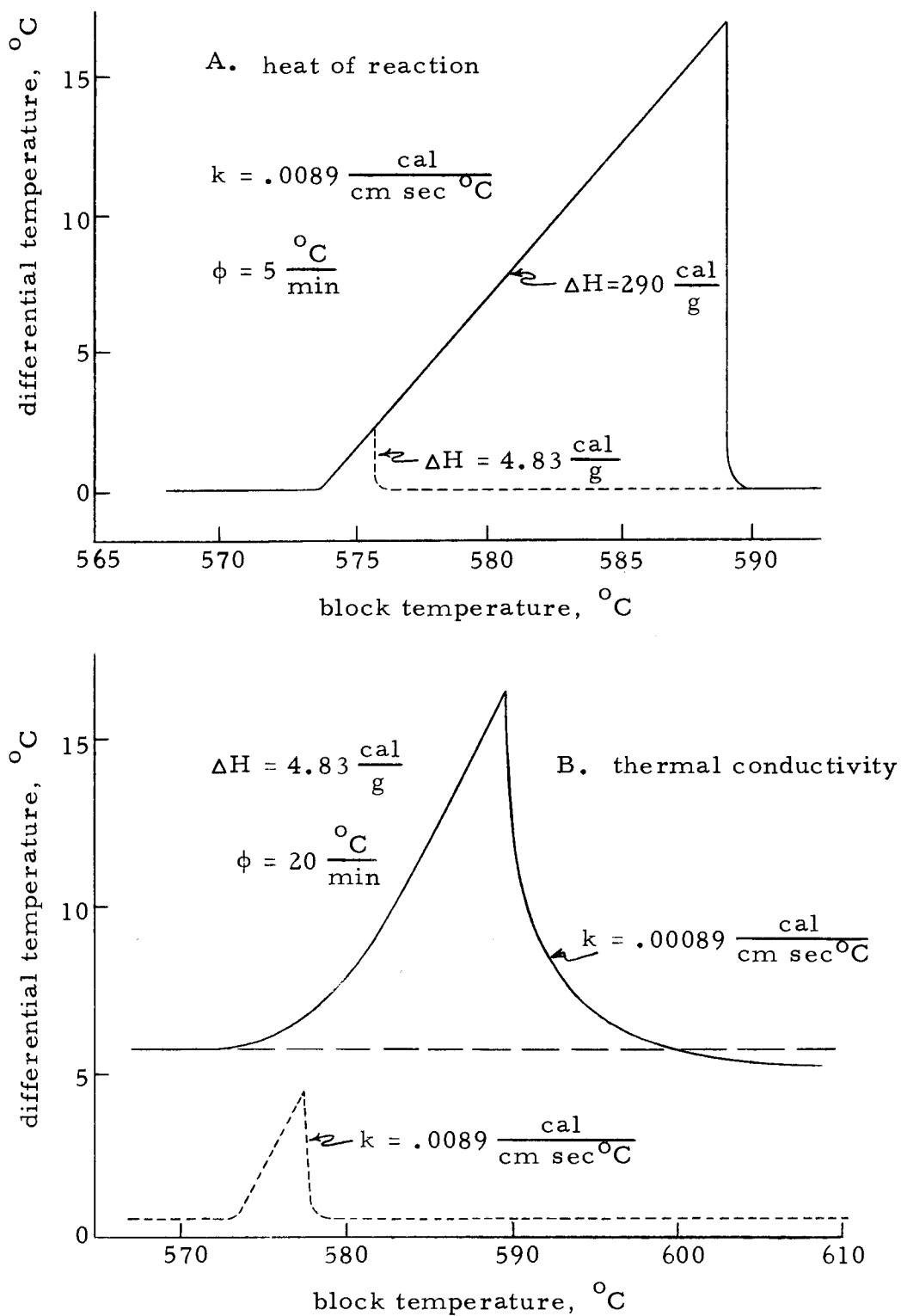


Figure 13. The effect of the thermal properties of the test sample upon peak shape.

thermal conductivity one tenth the value of the respective values used to generate the other peak in Figure 13b. Thus, since the curvature of this theoretical peak is more like the experimental cases when a lower conductivity is used, a possible conclusion is that the discrepancy between the experimental peaks and the present theoretical peaks lies in the error of the thermal conductivity of the model being too high. However, a reservation should be made that a future comparison with more explicit experimental DTA data giving actual  $\Delta T$ 's could corroborate this conclusion, or conversely, could reveal the importance of other effects such as block resistance.

The magnitude of the baseline shift predicted by the theoretical curves relative to the peak height is much less than the relative magnitude of the baseline shift shown by experimental curves. The exact cause of this discrepancy is not known, but it is expected that experimental errors such as drift in signal amplifiers or changing properties of thermocouples may contribute to this shift. Of course, if the thermal conductivity of the sample increases as a result of the reaction, this effect accounted for in the theoretical model would give a larger baseline shift than the present theoretical peaks. Hence, this is another case where the precise thermal conductivity of the quartz sample over the entire temperature range of interest is needed before the causes of one of the peak characteristics can be known.

One additional effect tested was that of the sample thermocouple's

thermal inertia and the thermal conduction. Upon adding a correction for these thermocouple effects to the model, it was found that these effects had no effect upon the curvature. However, it was found that for conductions away from the sample the slope of the rising portion of the peak decreased and the temperature at the top of the peak increased. In addition, inertial effects tended to increase the peak temperature but had no other noticeable effect upon the peak shape. For the thermocouple that was simulated (one which was made of platinum wire, 0.32 millimeters in diameter),<sup>7/</sup> the magnitude of the effects upon the peak temperature was less than one percent.

A negative result of the present work is that no improved way of determining the transition temperature from a DTA peak was found. This only corroborates a statement of Garn (15, p. 1560157), deduced from the work of Smyth (38), that the only two simple relationships between a peak and the transition temperature are first, that when the system temperature is measured in the block, the initial rise of the peak from the baseline corresponds to the transition temperature, and second, that when the system temperature is measured in the test sample, the maximum peak temperature corresponds to the transition temperature. Other connections between the peak and transition temperature are unclear.

---

<sup>7</sup>A specific description of the simulation of the thermocouples is given in Appendix V.

## CONCLUSIONS

A model was developed which utilizes fewer physical assumptions, and a more accurate mathematical treatment than previous models. The model is capable of predicting, semi-quantitatively, the experimental results for quartz. While the present model is by no means perfect, it does offer a new starting point and a direction for additional work, and it does show more clearly the principle parameters which dictate an experimental DTA curve. In addition previous work upon the improved use of DTA in quantitative studies to determine transition temperatures was corroborated.

A further conclusion upon the use of DTA in quantitative measurements can be made. Better success in measurements will result from careful experimental design: new apparatus being built to conform to theoretical considerations, rather than theory being developed to conform to existing apparatus. Three successful approaches, that of Borchardt and Daniels (6), that of Boersma (5), and that of Vassallo and Harden (46), exemplify this fact. In each of these studies completely new DTA apparatus were designed specifically to study particular variables, and in this way, the interference of competing effects upon the effect under study may be designed out of the experiment. However, in the cases where a new apparatus cannot be built, investigators at this time will have to be content to rely upon the relatively few, mainly qualitative theoretical DTA investigations presently published in order to make quantitative interpretations from differential thermal analysis peaks.

## RECOMMENDATIONS FOR FUTURE WORK

Much of the success of future work on a quantitative DTA model is contingent upon the existence of additional experimental data. Future work should possess accurate thermal conductivity data for the samples, for without this data any theoretical peak will have questionable quantitative accuracy. Additionally, experimental DTA peaks giving actual magnitudes of  $\Delta T$  and more specific descriptions of the experimental apparatus generating these peaks are needed in order to obtain a valid quantitative model.

Two areas in which the present model could be improved are the account of heat lag in the block and the account for the finite length of a cylindrical sample. The account of the heat lag in the block would generate a second finite difference solution for the block superimposed around the present one for the sample, and this would certainly be a formidable problem. Similarly, the account for the axial heat transfer in a finite length cylinder would greatly add to the complexities, particularly regarding the movement and shape of the phase boundary. Some suggestions for solving the finite cylinder problem are given in Appendix IV. Since both of these improvements would require a much larger number of calculations to achieve a numerical solution and since in the present model the present high speed computer was being used nearly to capacity as regards the

storage capacity and the computer cost of each program run, these improvements may be contingent upon the development of a much higher speed computer or upon the use of a more efficient approximate numerical method.

## BIBLIOGRAPHY

1. Arens, Pedro Laurent. A study of the differential thermal analysis of clays and clay minerals. Gravehage, Netherlands, Excelsiors Foto-Offset's, 1951. 131 p.
2. Barrall, Edward M., II, Roger S. Porter and Julian F. Johnson. Microboiling point determinations at 30 to 760 torr by differential thermal analysis. *Analytical Chemistry* 37:1053-1054. 1965.
3. Barrall, Edward M., II and L.B. Rogers. Differential thermal analysis of organic samples. Effects of geometry and operating variables. *Analytical Chemistry* 34:1101-1106. 1962.
4. Berkelhamer, Louis H. Differential thermal analysis of quartz. Washington, D.C., 1944. 18 p. (U.S. Bureau of Mines. Report of Investigations. R.I. 3763)
5. Boersma, S.L. A theory of differential thermal analysis and new methods of measurement and interpretation. *Journal of The American Ceramic Society* 38:281-284. 1955.
6. Borchardt, Hans J. and Farrington Daniels. The application of differential thermal analysis to the study of reaction kinetics. *Journal of the American Chemical Society* 79:41-46. 1957.
7. Carslaw, H.S. and J.C. Jaeger. Conduction of heat in solids. 2d ed. Oxford, Clarendon, 1959. 510 p.
8. Control Data Corporation. 3100, 3200, 3300, 3500 computer systems FORTRAN reference manual. Palo Alto, Control Data, 1966. Various paging.
9. Crank, J. Two methods for the numerical solution of moving-boundary problems in diffusion and heat flow. *Quarterly Journal of Mechanics and Applied Mathematics* 10:220-231. 1957.
10. Crank, J. and P. Nicolson. A practical method for numerical evaluation of solutions of partial differential equations of the heat-conduction type. *Proceedings of the Cambridge Philosophical Society* 43:50-67. 1947.
11. Douglas, Jim, Jr. A survey of numerical methods for parabolic differential equations. *Advances in Computers* 2:1-54. 1961.



12. Dufort, E.C. and S.P. Frankel. Stability conditions in the numerical treatment of parabolic differential equations. *Mathematical Tables and Other Aids to Computation* 7:135-152. 1953.
13. Dusinberre, George Merrick. Heat-transfer calculations by finite differences. Scranton, International Textbook, 1961. 293 p.
14. Forsythe, George E. and Wolfgang G. Wasow. Finite-difference methods for partial differential equations. New York, Wiley, 1960. 444 p.
15. Garn, Paul D. Thermoanalytical methods of investigation. New York, Academic, 1965. 606 p.
16. Goldsmith, Alexander, Thomas E. Waterman and Harry J. Hirschhorn (comps.). Handbook of thermophysical properties of solid materials. Vol. 3, Rev. ed. New York, Pergamon, 1961. 1162 p.
17. Grim, R.E. and R.A. Rowland. Differential thermal analysis of clay materials and other hydrous materials. *The American Mineralogist* 27:746-761, 801-818. 1942.
18. Hodgman, Charles D., Robert C. Weast and Samuel M. Selby (eds.). Handbook of chemistry and physics. 42d. ed. Cleveland, Chemical Rubber, 1960. 3481 p.
19. Jakob, Max. Heat transfer. Vol. 1. New York, Wiley, 1949. 758 p.
20. Kaplan, Wilfred. Advanced calculus. Reading, Mass., Addison-Wesley, 1956. 679 p.
21. Keith, M.L. and O.F. Tuttle. Significance of variation in the high-low inversion of quartz. *American Journal of Science*, Bowen volume, p. 203-280. 1952.
22. Kissinger, Homer E. Reaction kinetics in differential thermal analysis. *Analytical Chemistry* 29:1702-1706. 1957.
23. \_\_\_\_\_ . Variation of peak temperature with heating rate in differential thermal analysis. *Journal of Research of the National Bureau of Standards* 57:217-221. 1956.

24. Kreith, Frank. Principles of heat transfer. Scranton, International Textbook, 1958. 553 p.
25. Kronig, R. and F. Snoodÿk. On the determination of heats of transformation in ceramic materials. Applied Scientific Research, sec. A, 3:27-30. 1953.
26. Lapidus, Leon. Digital computation for chemical engineers. New York, McGraw-Hill, 1962. 407 p.
27. Larkin, Bert K. Some finite difference methods for problems in transient heat flow. In: Heat transfer - Cleveland. New York, American Institute of Chemical Engineers, 1965. p. 1-11. (Chemical Engineering Progress Symposium series, Vol. 61, No. 59)
28. McAdams, William. Heat transmission. 3d ed. New York, McGraw-Hill, 1954. 532 p.
29. Mackenzie, Robert C. Thermal methods. In: The differential thermal analysis of clays. London, Mineralogical Society, 1957. p. 1-22.
30. Milne, William Edward. Numerical calculus. Princeton, N. J., Princeton University, 1949. 393 p.
31. Murray, P. and J. White. Kinetics of the thermal dehydration of clays. Part IV. Interpretation of the differential thermal analysis of the clay minerals. Transactions of the British Ceramic Society 54:204-238. 1955.
32. Organick, Elliot I. A FORTRAN primer. Reading, Mass., Addison-Wesley, 1963. 186 p.
33. Reed, Ronald L., Leon Weber and Byron S. Gottfried. Differential thermal analysis and reaction kinetics. Industrial and Engineering Chemistry Fundamentals 4:38-46. 1965.
34. Schneider, Paul J. Conduction heat transfer. Cambridge, Mass., Addison-Wesley, 1955. 395 p.
35. Sewell, E.C. and D.B. Honeyborne. Theory and quantitative use. In: The differential thermal analysis of clays, ed. by Robert C. Mackenzie. London, Mineralogical Society, 1957. p. 65-97.

36. Smith, W. The thermal conductivity of dry soil. *Soil Science* 53:435-459. 1942.
37. Smothers, W.J. and Yao Chiang. *Handbook of differential thermal analysis*. New York, Chemical Publishing, 1966. 633 p.
38. Smyth, Harold T. Temperature distribution during mineral inversion and its significance in differential thermal analysis. *Journal of The American Ceramic Society* 34:221-224. 1951.
39. Soulé, J.L. Quantitative interpretation of differential thermal analysis. *Journal of Physical Radium* 13:516-520. 1952.
40. Speil, Sidney. Applications of thermal analysis to clays and aluminous minerals. In: *Differential thermal analysis. Its application to clays and other aluminous materials*. Wasington, D.C. 1945. p. 1-37. (U.S. Bureau of Mines. Technical Paper 644)
41. Speros, D.M. and R.L. Woodhouse. Realization of quantitative differential thermal analysis. I. Heats and rates of solid-liquid transitions. *The Journal of Physical Chemistry* 67:2164-2168. 1963.
42. Strella, Stephan. Differential thermal analysis of polymers. I. The glass transition. *Journal of Applied Polymer Science* 7:569-579. 1963.
43. \_\_\_\_\_ . Differential thermal analysis of polymers. II. Melting. *Journal of Applied Polymer Science* 7:1281-1289. 1963.
44. Trench, William F. On an explicit method for the solution of a Stephan problem. *Journal of the Society of Industrial and Applied Mathematics* 7:184-204. 1959.
45. Tsang, N.F. Theoretical background in quantitative DTA. In: *Handbook of differential thermal analysis*, by W.J. Smothers and Yao Chiang. New York, Chemical Publishing, 1966. p. 90-122.
46. Vassallo, D.A. and J.C. Harden. Precise phase transition measurements of organic materials by differential thermal analysis. *Analytical Chemistry* 34:132-135. 1962.

47. Vold, Marjorie J. Differential thermal analysis. *Analytical Chemistry* 21:683-688. 1949.
48. Wendlandt, W.W. Differential thermal analysis. In: *Technique of inorganic chemistry*, ed. by Hans B. Jonassen and Arnold Weissberger. Vol. 1. New York, Interscience, 1963. p. 209-257.
49.                     . Thermal methods of analysis. New York, Interscience, 1964. 424 p.
50. Wicks, C.E. and F.E. Block. Thermodynamic properties of 65 elements - their oxides, halides, carbides, and nitrides. Washington, D.C., 1963. 146 p. (U.S. Bureau of Mines. Bulletin 605)
51. Williamson, E.D. and L.H. Adams. Temperature distribution in solids during heating and cooling. *Physical Review*, ser. 2, 14:99-114. 1919.

## APPENDICES

## APPENDIX I

## Nomenclature

<u>Symbol</u>	<u>Definition</u>	<u>Units</u>
A	Area of heat transfer	cm <sup>2</sup>
A <sub>b</sub>	Area of boundary def. by [57b]	cm <sup>2</sup>
A <sub>e</sub>	Area of heat transfer def. by [57c]	cm <sup>2</sup>
A <sub>f</sub>	Area of heat transfer def. by [57a]	cm <sup>2</sup>
a	Outer radius of cylinder	cm
a	Limit of integration in [9]	sec
a <sub>j</sub>	Interpolation parameter (see [14])	
c	Specific heat capacity	$\frac{\text{cal}}{\text{g}^{\circ}\text{C}}$
c	Limit of integration in [9]	sec
f	Void fraction def. by the equation at the top of page 39.	
f( )	Interpolated function	
g	Geometrical shape constant in [9]	
ΔH	Latent heat of phase change	$\frac{\text{cal}}{\text{g}}$
J <sub>0</sub>	Bessel function of zero order	
J <sub>1</sub>	Bessel function of first order	
K	Total number of cylindrical shells = $\frac{a}{\Delta x}$	
k	Thermal conductivity	$\frac{\text{cal}}{\text{sec cm}^{\circ}\text{C}}$
k <sub>1</sub>	Thermal conductivity of high form of quartz	$\frac{\text{cal}}{\text{sec cm}^{\circ}\text{C}}$
k <sub>2</sub>	Thermal conductivity of low form of quartz	$\frac{\text{cal}}{\text{sec cm}^{\circ}\text{C}}$
k <sub>s</sub>	Thermal conductivity of solid material	$\frac{\text{cal}}{\text{sec cm}^{\circ}\text{C}}$
ℓ	Time increments since beginning of phase change	

<u>Symbol</u>	<u>Definition</u>	<u>Units</u>
$l$	Half-thickness of slab in [7]	cm
$l_j$	Def. by [15]	
$M$	Def. by $\frac{\Delta x^2}{\alpha \Delta t}$	
$M$	Mass of active material in [9]	g
$m$	Specifies a radial distance ( $x = m\Delta x$ )	
$n$	Specifies a time ( $t = n\Delta t$ )	
$P_n$	Def. by [16]	
$p$	Geometric ratio shown in Figure 5	
$q$	Rate of heat flow	cal/sec
$r$	Radial cylindrical coordinate	cm
$S$	Transition boundary thickness	cm
$T$	Temperature	$^{\circ}\text{C}$
$T_m^n$	Temperature at position $m\Delta x$ at time $n\Delta t$	$^{\circ}\text{C}$
$T_o$	Initial temperature	$^{\circ}\text{C}$
$T_L$	Transition temperature	$^{\circ}\text{C}$
$\Delta T$	Differential temperature	$^{\circ}\text{C}$
$t$	Time	sec
$\Delta t$	Time increment	sec
$V$	Volume	$\text{cm}^3$
$x$	Distance coordinate	cm
$x(t)$	Radial location of boundary at $t$	cm
$x(n\Delta t)$	Same as $x(t)$	cm



<u>Symbol</u>	<u>Definition</u>	<u>Units</u>
$\Delta x$	Distance increment	cm
$\delta x$	Boundary movement during $\Delta t$	cm
$y$	Distance coordinate	cm
$z$	Distance coordinate	cm

### Greek Symbols

$\alpha$	Thermal diffusivity = $\frac{k}{\rho c}$	$\text{cm}^2/\text{sec}$
$\alpha$	Low phase of quartz	
$\beta$	High phase of quartz	
$\beta_n$	$n^{\text{th}}$ root of $J_0(\alpha\beta_n) = 0$	$\text{cm}^{-1}$
$\theta$	Angular coordinate	radians
$\rho$	Density	$\text{g}/\text{cm}^3$
$\phi$	Heating rate	$^{\circ}\text{C}/\text{sec}$

### Miscellaneous Symbols

$\partial$	Signifies partial derivative	
$d$	Signifies total derivative	
$\nabla^2$	Laplacian def. by [2] and [3]	$\text{cm}^{-2}$
$O(\ )$	Order of the error in a finite difference approximation (see page 43)	
$\left. \begin{array}{l} n \\   \\ m \end{array} \right\}$	Signifies a derivative evaluated at $x = m\Delta x$ at $t = n\Delta t$	

## APPENDIX II

### Two Explicit Finite Difference Methods

Dufort and Frankel Method

Exponential Method of Larkin

### Two Explicit Finite Difference Methods

The specific finite difference equations of radial heat conduction in a cylinder for the Dufort and Frankel method (12) and for the exponential method described by Larkin (27) will be given. If the gradient of the heat Equation 4 is replaced by a finite difference approximation the result may be written as

$$\left. \frac{\partial T}{\partial t} \right|_m^n = \alpha \frac{\frac{2m+1}{2m} T_{m+1}^n - 2T_m^n + \frac{2m-1}{2m} T_{m-1}^n}{\Delta x^2} \quad (\text{II-1})$$

This equation will be the starting point in describing each of the two methods.

#### Dufort and Frankel Method

The Dufort and Frankel method results from two modifications of Equation II-1. First, the time derivative is replaced by a three-point central difference expression, and second, the temperature  $T_m^n$  is replaced by

$$\frac{T_m^{n+1} + T_m^{n-1}}{2}$$

in order to improve stability. The result, if  $m \neq 0$  is

$$\frac{T_m^{n+1} - T_m^{n-1}}{2\Delta t} = \alpha \frac{\frac{2m+1}{2m} T_{m+1}^n - T_m^{n+1} - T_m^{n-1} + \frac{2m-1}{2m} T_{m-1}^n}{\Delta x^2}. \quad (\text{II-2})$$

Equation II-2 can be rearranged to

$$T_m^{n+1} = T_m^{n-1} + \frac{2}{M+2} \left( \frac{2m+1}{2m} T_{m+1}^n - 2T_m^{n-1} + \frac{2m-1}{2m} T_{m-1}^n \right). \quad (\text{II-3})$$

Note that the Dufort and Frankel method requires the initial conditions at two time steps,  $n$  and  $n-1$ , to begin calculations. For the special case where  $m = 0$  the result is

$$T_0^{n+1} = T_0^{n-1} + \frac{8}{M+4} (T_1^n - T_0^{n-1}). \quad (\text{II-4})$$

### Exponential Method of Larkin

The exponential method of Larkin results from the integration of Equation II-2 with respect to time with  $T_m$  allowed to vary and with  $T_{m+1}^n$  and  $T_{m-1}^n$  held constant. The result of integrating Equation II-1 with respect to time from  $n\Delta t$  to  $(n+1)\Delta t$ , if  $m \neq 0$ , is

$$T_m^{n+1} = z T_m^n + (1-z) \left( \frac{2m+1}{4m} T_{m+1}^{n+1} + \frac{2m-1}{4m} T_{m-1}^n \right) \quad (\text{II-5})$$

where

$$z = e^{-\left(\frac{2}{M}\right)}.$$

Note that calculations using this exponential method need to begin at a boundary where a  $T_K^{n+1}$  is known, and then  $m$  is decreased by one for each subsequent calculation during a single time step. The special case for  $m = 0$  has the result as

$$T_0^{n+1} = T_0^n z' + (1-z')T_1^n \quad (\text{II-6})$$

where

$$z' = e^{-\left(\frac{4}{M}\right)} .$$

## APPENDIX III

## Computer Programs

Computer Program Nomenclature

Flow Chart Symbols

Flow Chart

Computer Programs (in pocket on back cover)

Two-Point Equations Including Graphical plot

Three-Point Equations

Computer Program Nomenclature






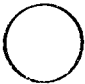
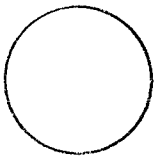
<u>Computer Symbol</u>	<u>Meaning</u>
CON	k
CON1	$k_1$
CON2	$k_2$
DELTT	$\Delta T$
DELTX	$\delta x$
DIF1	$a_1$
DIF2	$a_2$
DT	$\Delta t$
DX	$\Delta x$
INTER	Number of calculational cycles between print-outs
ITE	Maximum number of calculational cycles before END
K	$K + 10$
M	$m + 10$
ML	Value of $m + 10$ containing the phase boundary
N	$n + 10$
NL	$n + 10$
P	p
PHI	$\phi$
REM1	$\frac{1}{M_1} = a_1 \Delta t / \Delta x^2$

<u>Computer Symbol</u>	<u>Meaning</u>
REM2	$\frac{1}{M_2} = a_2 \Delta t / \Delta x^2$
RRL	$\frac{1}{\rho \Delta H}$
T(M, N)	$T_m^n$
TIME	t
TL	$T_L$
X(NL)	x(t), x(nΔt)
XT	a = KΔx

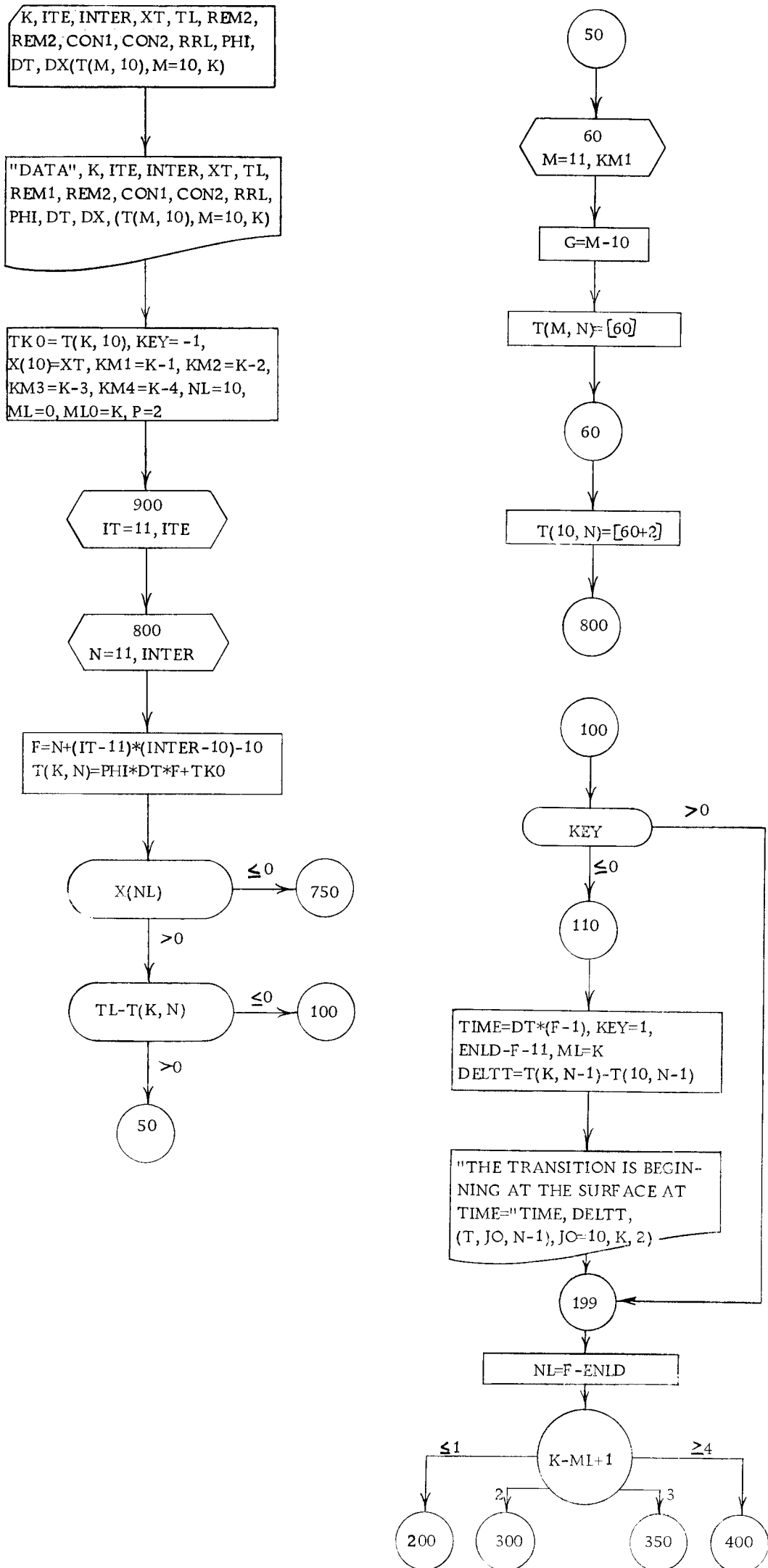


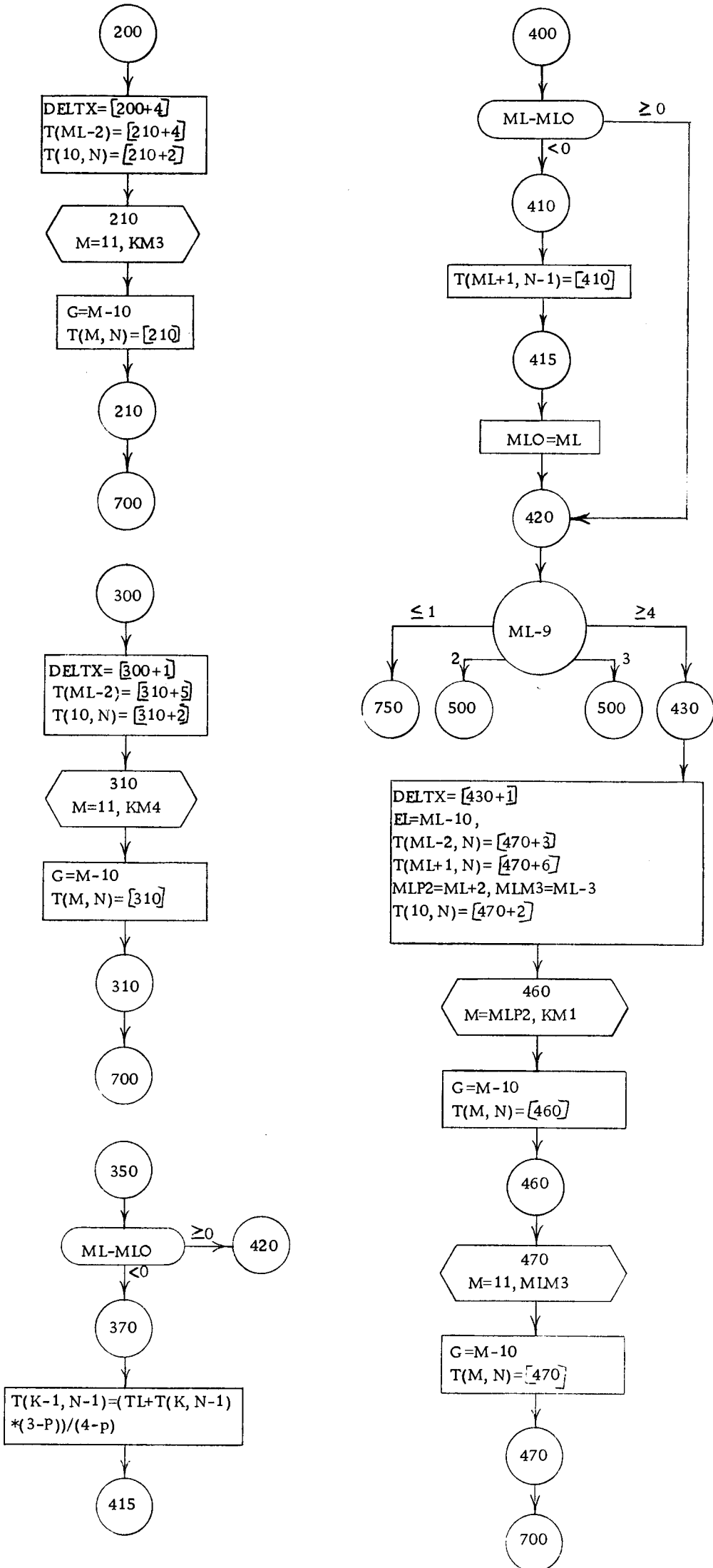
### Flow Chart Symbols

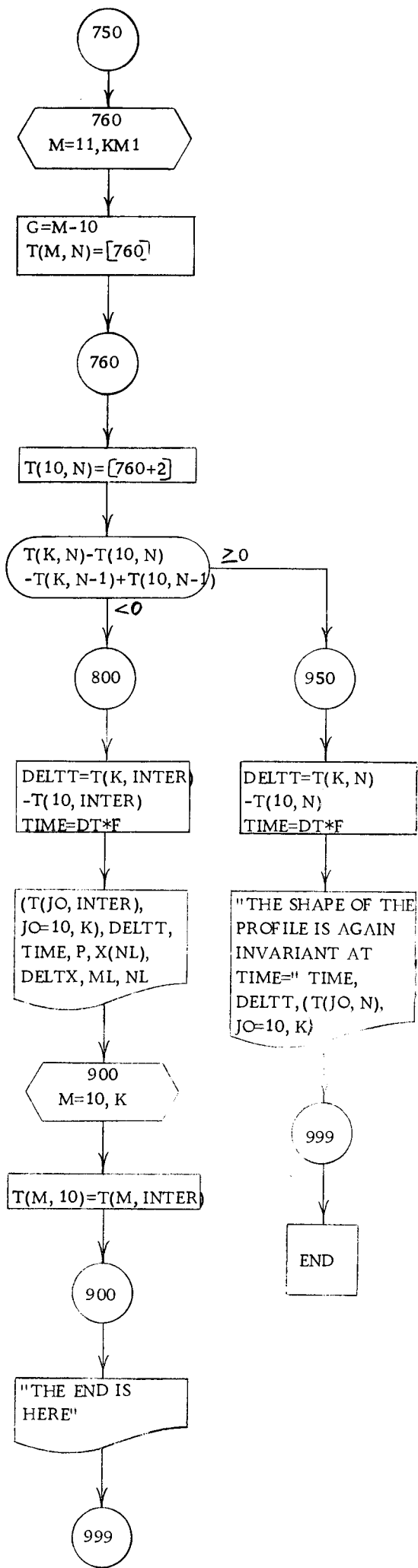
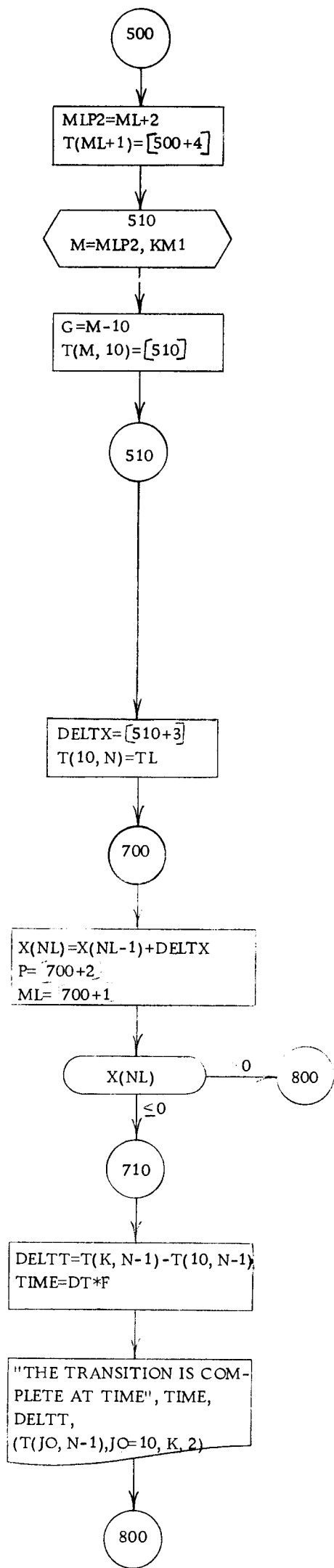
The flow chart on the ensuing pages graphically represents the FORTRAN computer program which follows the flow chart. For equations too long to be printed out in a box on the flow chart, the numbers appearing in brackets specify the equations in the program by statement numbers plus, if needed, the numbers of lines beyond these statement numbers. Note that the plotting functions have been omitted in this flow chart. The flow chart conventions are the same ones used by Organick (32, p. 169):

<u>Symbol</u>	<u>Meaning</u>	<u>Symbol</u>	<u>Meaning</u>
	READ		DO Loop
	PRINT		Calculation
	IF		Connection
	GO TO		

Flow Chart







## APPENDIX IV

## A Finite-Length Cylindrical Sample

Figure A-1. Grid and moving boundary within a finite-length cylinder.

### A Finite-Length Cylindrical Sample

Suggestions for treating a finite-length cylindrical sample will be presented based upon the observations made during the course of this work. No actual complete calculations for a moving phase boundary were made in this study, but these observations are included as they could be useful in future investigations.

Finite difference equations were derived which described the profile within the sample by approximating a solution to the heat Equation 21. The general case, where  $l \neq 0$  and  $m \neq 0$  for the grid shown in Figure A-1 ( $l$  specifies a distance  $z = l \Delta z$ ), can be written as

$$\frac{T_{l,m}^{n+1} - T_{l,m}^n}{\Delta t} = \alpha \left[ \frac{T_{l,+1,m}^n - 2T_{l,m}^n + T_{l-1,m}^n}{\Delta z^2} + \frac{\frac{2m+1}{2m} T_{l,m+1}^n - 2T_{l,m}^n + \frac{2m-1}{2m} T_{l,m-1}^n}{\Delta x^2} \right] \quad (\text{IV-1})$$

Equation IV-1 can be solved for  $T_{l,m}^{n+1}$ , and the special case when  $\Delta z = \Delta x$  gives

$$T_{l,m}^{n+1} = T_{l,m}^n + \frac{1}{M} \left[ T_{l+1,m}^n + T_{l-1,m}^n + \frac{2m+1}{2m} T_{l,m+1}^n + \frac{2m-1}{2m} T_{l,m-1}^n - 4T_{l,m}^n \right] \quad (\text{IV-2})$$

When  $m = 0$  and  $l \neq 0$ , the result is

$$T_{l,0}^{n+1} = T_{l,0}^n + \frac{1}{M} \left[ 4T_{l,1}^n + T_{l+1,0}^n + T_{l-1,0}^n - 6T_{l,0}^n \right], \quad (\text{IV-3})$$

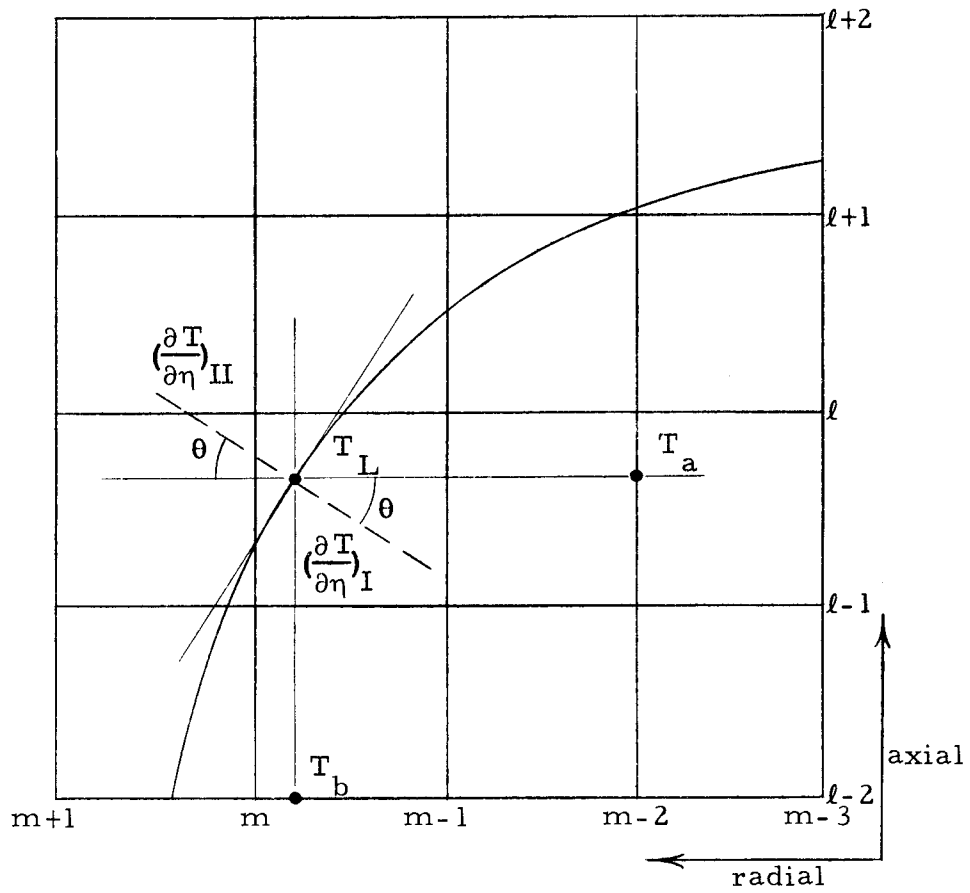


Figure A-1. Grid and moving boundary within a finite-length cylinder.

and when  $m \neq 0$  and  $\ell = 0$ , the result is

$$T_{0,m}^{n+1} = T_{0,m}^n + \frac{1}{M} \left[ 2T_{1,m}^n + \frac{2m+1}{2m} T_{0,m+1}^n + \frac{2m-1}{2m} T_{0,m-1}^n - 4T_{0,m}^n \right]. \quad (\text{IV-4})$$

Finally, when  $m = 0$  and  $\ell = 0$ , the equation for  $T_{0,0}^{n+1}$  is

$$T_{0,0}^{n+1} = T_{0,0}^n + \frac{1}{M} \left[ 4T_{0,1}^n + 2T_{1,0}^n - 6T_{0,0}^n \right]. \quad (\text{IV-5})$$

Equations IV-2 through IV-5 were used to find the temperature profile in a cylinder with a length of twice the diameter, and with the same thermal properties used by Tsang (45). The computer running time became so long, and consequently so expensive for a 20 x 40 segment grid, that plans for further calculations involving a finite-length cylinder were suspended. The reason for this long computer running time is that 861 temperatures need to be calculated during each time step for this two-dimensional grid instead of 21 temperatures for the infinite cylinder. In addition, the stability criteria are more stringent for the finite cylinder (11), and thus a smaller  $\Delta t$  is required.

The mathematical analysis required to describe the movement of the phase boundary in a finite-length cylinder is much more complex than the same description in an infinite cylinder. This increased complexity results from the temperature gradient at the boundary being caused by a component in the axial direction in addition to a



component in the radial direction. Consequently, the gradient and the rate of the boundary movement during a time step is a function of the location along the boundary. Thus several equations are needed to describe the changing location of the boundary during each time step.

One of these equations specifying the movement of a certain point on the boundary will be described. The entire boundary can be approximated by straight line segments connecting several of these points lying on the boundary. The movement of the boundary will be in a direction  $\eta$ , normal to the boundary, and will have a magnitude described by

$$\delta\eta = \frac{\Delta t}{\rho \Delta H A_b} \left[ -k_I A_I \left( \frac{\partial T}{\partial \eta} \right)_I + k_{II} A_{II} \left( \frac{\partial T}{\partial \eta} \right)_{II} \right] \quad (\text{IV-6})$$

where  $A_b, A_I$ , and  $A_{II}$  are functions of the radial distance as in the infinite cylindrical model. Note the correspondence between Equation IV-6 and Equation 28; only the direction is different.

The determinations of the gradients,  $\left( \frac{\partial T}{\partial \eta} \right)_I$  and  $\left( \frac{\partial T}{\partial \eta} \right)_{II}$ , shown in Figure A-1, are complex. Lapidus (26, p. 155) gives a form for such a gradient as

$$\frac{\partial T}{\partial \eta} = \frac{\partial T}{\partial x} \cos \theta + \frac{\partial T}{\partial y} \sin \theta \quad (\text{IV-7})$$

where  $\theta$  is the angle of the normal to the boundary from the

horizontal as shown in Figure A-1. The direction of  $\frac{\partial T}{\partial \eta}$  can be found by using Lagrange's interpolation equation (26, p. 36-41) to determine the equation for the curved boundary at a fixed time and then by taking the negative of the distance derivative of this equation. Evaluating this equation at a point on the boundary gives the slope of a normal to the boundary. The magnitude of  $\frac{\partial T}{\partial x}$  and  $\frac{\partial T}{\partial y}$  can be found applying difference approximations like those used in the one-dimensional model, but the resulting equations are involved. It can be seen that the treatment of a moving boundary in a two-dimensional case has complications not existing in one dimension.

APPENDIX V

Thermocouple Effects

Heat Conduction

Thermal Inertia

### Thermocouple Effects

Thermocouple effects can be estimated by accounting for the heat conduction and the thermal inertia of a thermocouple in the center of a sample. The only change in the equations for the model occurs in Equation 36 describing the center temperature. An additional term is added to Equation 36 to account for the thermocouple's heat conduction, and only a change in the diffusivity used in Equation 36 is needed to account for the thermocouple's thermal inertia.

#### Heat Conduction

The correction for heat conduction in a thermocouple can be made by considering a heat balance about the center of the sample. Consider the construct in Figure 5. The center-most section, 0, is a cylinder of a radius  $\Delta x/2$  containing the thermocouple at a temperature,  $T_0^n$ ; and the next section, 1, is a cylindrical shell of thickness  $\Delta x$  of temperature  $T_1^n$ . The thermocouple will be considered to be a line at the center of the infinite cylinder acting as a heat sink. Consequently, the equation for  $T_0^{n+1}$  will contain a term for the thermocouple's heat conduction out of the central segment. An energy balance for the central segment can be written as

$$\rho CV \frac{dT}{dt} = -kA \frac{dT}{dx} + q_t \quad (V-1)$$

energy accumulation      heat conduction in      heat conduction in  
    through the sample      via the thermocouple

where  $\rho$ ,  $C$ , and  $k$  are properties of the sample. In finite difference form, Equation V-1 for a unit length of the cylinder in Figure 5 becomes

$$\rho C \left[ \pi \left( \frac{\Delta x}{2} \right)^2 (1) \right] \frac{T_0^{n+1} - T_0^n}{\Delta t} = -k [\pi (\Delta x) (1)] \frac{dT}{dx} + q_t \quad (V-2)$$

Rearranging Equation V-2 gives

$$T_0^{n+1} = T_0^n + \frac{4}{M} \left( T_1^n - T_0^n + \frac{q_t}{\pi k} \right) \quad (V-3)$$

Thus, provided  $q_t$  can be found, Equation V-3 can be used to calculate  $T_0^{n+1}$ , thus accounting for the thermocouple conduction.

The estimation of the rate of thermocouple heat conduction,  $q_t$ , can be made by using a variation of Fourier's Equation 23 as

$$q_t = k_t A_t \frac{T_D - T_t}{D} \quad (V-4)$$

where

$k_t$  = the thermal conductivity of the thermocouple metal,

$A_t$  = the cross-sectional area of the thermocouple wires,

$T_t$  = the temperature measured by the thermocouple,

$T_D$  = some datum temperature of the wires away from the center  
of the sample,

and  $D$  = the distance along the wires between  $T_I$  and  $T_t$ .

The actual determination of  $T_D$  seems very difficult, but the present discussion offers an estimate of  $T_D$  and  $D$  so that the order of magnitude of  $q_t$  may be ascertained. Boersma (5) states that the thermocouple wires will have reached the block temperature at a very short distance from the point at which the wires have left the sample and have entered the block. This implies that in the present case  $T_I - T_t \cong 5^\circ\text{C}$  and  $D \cong 1.4$  cm (from Figure 4). For platinum thermocouple wires, where  $k \cong .1 \frac{\text{cal}}{\text{cm sec}^\circ\text{C}}$  (18, p. 2435), of radius .032 cm,  $q_t$  was found as

$$q_t \cong .1 \times \frac{\pi(.032)^2}{4} \times \frac{5}{1.4} = 2.87 \times 10^{-4} \frac{\text{cal}}{\text{sec}}. \quad (\text{V-5})$$

When a value of  $q_t$  of  $-.00252 \frac{\text{cal}}{\text{sec}}$  was used, the difference in the values of the differential temperature between this case and the case where the thermocouple effects were ignored was only 0.14%.

Since the absolute value of  $q_t$  was much larger than that calculated

above, the effect of  $q_t$  calculated in Equation V-5 would be negligible.

### Thermal Inertia

Accounting for the thermal inertia for the thermocouple is relatively simple. This only requires the use of a different value of  $M$  in Equation 36 to account for the thermal properties of the thermocouple being different from those of the sample. This correction entails assuming the thermocouple to be negligible in size compared to the sample as regards the phase change—an assumption which is physically tenable. As in the case of thermocouple heat conduction, the effect of thermal inertia of the thermocouple was negligible in the present model.

FORTRAN Computer Program Employing  
Two-Point Finite Difference Equations and Plotter Subroutines

```
'SEQUENCE,500,          CHEMICAL ENGINEERING      JOHN KAAKINEN
'JOB,75038RMJK , JWK ,100,
'EQUIP,10=MTC1E0U01
'CTO,SAVE TAPE FROM UNIT 1 FOR PLOTTING
'FORTRAN,L,X
PROGRAM INFCYL2
DIMENSION T(30,130),X(130)
DO 1200 LES=1,3
READ 10,K,ITE,INTER,PHI,DT,DX,DIF1,DIF2,CON,RRL,TL,(T(M,10),M=10,K
1)
10 FORMAT(3I4,3F12.8/ 5F12.8/6F12.7/5F12.7)
XT=DX*(K-10)
PHIM=60*PHI
REM1=DT*DIF1/DX**2      $REM2=DT*DIF2/DX**2
EM1=1/REM1      $ EM2=1/REM2
PRINT 20,K,ITE,INTER,PHI,PHIM,DT,DX,DIF1,DIF2,EM1,EM2,TL,XT,CON,RR
1L,(T(M,10),M=10,K)
20 FORMAT(50X,4HDATA/4H K=I4,5H ITE=I4,7H INTER=I4,5H PHI=F9.6,8HDEG
1/SEC=F6.2,12HDEG/MIN DT=F10.8,4H DX=F10.8/7H DIF1=F12.8,6H DIF2=
2F12.8,4H M1=F12.8,4H M2=F12.8,4H TL=F6.2,4H XT=F6.4,5H CON=F8.4,5H
2 RRL=F8.4/36H THE INITIAL TEMPERATURE PROFILE = 7F12.7/10F12.7/10
1F12.7/10F12.7/4F12.7)
DELTS1=.25*PHI*XT**2/DIF1  $ DELTS2=.25*PHI*XT**2/DIF2
DELTA=22.3*PHI*XT**2
PRINT 30,DELTS1,DELTS2,DELTA
30 FORMAT(/9H DELTS1=F12.7,9H DELTS2=F12.7,8H DELTA=F12.7//)
DO 35 L=10,INTER
35 X(L)=XT
CON1=CON2=CON
QT=0
PI=3.14159
TK0=T(K,10)
CALL AXISXY(10,8,5,1.,50.,6.,550.,0.,TK0,0.,.2,5)
CALL PLOTXY(TK0,0.,1,0)
KEY=-1
KM1=K-1  $ KM2=K-2  $ KM3=K-3  $ KM4=K-4
P=ML=DELTX=LL=0
MLO=K
DO 900 IT=11,ITE
DO 800 N=11,INTER
F=N+(IT-11)*(INTER-10)-10
T(K,N)=PHI*DT*F+TK0
NL=N
IF(X(NL)) 750,750,40
40 IF(TL-T(K,N)) 100,100,50
50 DO 60 M=11,KM1
```



```

G=M-10
60 T(M,N)=((1.-.5/G)*T(M-1,N-1)+(1.+5/G)*T(M+1,N-1))*REM2+(1.-2.*REM
12)*T(M,N-1)
T(10,N)=T(10,N-1)+4*REM2*(T(11,N-1)-T(10,N-1)+QT/PI/CON)
GO TO 800
100 IF (KEY) 110,110,199
110 TIME=DT*(F-1)
DELTT=T(K,N-1)-T(10,N-1)
PRINT 120,TIME,DELTT,(T(JO,N-1),JO=10,K)
120 FORMAT(/55H THE TRANSITION IS BEGINNING AT THE SURFACE AT TIME =
1F11.6,16H SECONDS DELTT=F12.7/12H TEMP = 10F12.7/11F12.7/10F1
22.7/10F12.7)
P=2
ML=K
KEY=1
ENLD=F-1
199 LL=F-ENLD
GO TO (200,300,350,400),K-ML+1
200 CONTINUE
D=-DT*RRL/X(NL-1)
E=CON1*.5*(XT+X(NL-1))*PHI*(LL-.5)*DT
H=CON2/P*(TL-T(ML-2,N-1))*(X(NL-1)-.5*P*DX)/DX*D
DELTX=XT-X(NL-1)-.5*H-SQRT((XT-X(NL-1)-.5*H)**2-2*(D*E-H*(XT-X(NL-
11))))
DO 210 M=11,KM3
G=M-10
210 T(M,N)=((1.-.5/G)*T(M-1,N-1)+(1.+5/G)*T(M+1,N-1))*REM2+(1.-2.*REM
12)*T(M,N-1)
T(10,N)=T(10,N-1)+4*REM2*(T(11,N-1)-T(10,N-1)+QT/PI/CON)
T(ML-1,N)=0
T(ML-2,N)=T(ML-2,N-1)+REM2*((TL-T(ML-2,N-1))*(X(NL-1)/P-.5*DX)-(T(
1ML-2,N-1)-T(ML-3,N-1))*(X(NL-1)-(P+.5)*DX))/((P+1)*X(NL-1)-DX*(.75
2*P**2+P+.25))
GO TO 700
300 CONTINUE
DELTX=-DT*RRL/(X(NL-1)*DX)*(CON1*PHI*(LL-.5)*DT/(3-P)*.5*(XT+X(NL-
11))-CON2*(TL-T(ML-2,N-1))*(X(NL-1)/P-.5*DX))
DO 310 M=11,KM4
G=M-10
310 T(M,N)=((1.-.5/G)*T(M-1,N-1)+(1.+5/G)*T(M+1,N-1))*REM2+(1.-2.*REM
12)*T(M,N-1)
T(10,N)=T(10,N-1)+4*REM2*(T(11,N-1)-T(10,N-1)+QT/PI/CON)
T(ML,N)=0
T(ML-1,N)=0
T(ML-2,N)=T(ML-2,N-1)+REM2*((TL-T(ML-2,N-1))*(X(NL-1)/P-.5*DX)-(T(
1ML-2,N-1)-T(ML-3,N-1))*(X(NL-1)-(P+.5)*DX))/((P+1)*X(NL-1)-DX*(.75
2*P**2+P+.25))
GO TO 700
350 IF (ML-ML0) 370,420,420
370 T(K-1,N-1)=(TL+T(K,N-1)*(3-P))/(4-P)
GO TO 415
400 IF (ML-ML0) 410,420,420
410 T(ML+1,N-1)=(P-3)/(5-P)*T(ML+3,N-1)+2*(P-3)/(P-4)*T(ML+2,N-1)+2/((
1P-5)*(P-4))*TL
415 ML0=ML
420 GO TO (750,500,500,430),ML-9
430 CONTINUE
DELTX=-DT*RRL/(X(NL-1)*DX)*(CON1*(T(ML+1,N-1)-TL)*(X(NL-1)/(3-P)+
15*DX)-CON2*(TL-T(ML-2,N-1))*(X(NL-1)/P-.5*DX))
MLP2=ML+2

```

```

DO 460 M=MLP2,KM1
G=M-10
460 T(M,N)=((1.-.5/G)*T(M-1,N-1)+(1.+5/G)*T(M+1,N-1))*REM1+(1.-2.*REM
11)*T(M,N-1)
MLM3=ML-3
DO 470 M=11,MLM3
G=M-10
470 T(M,N)=((1.-.5/G)*T(M-1,N-1)+(1.+5/G)*T(M+1,N-1))*REM2+(1.-2.*REM
12)*T(M,N-1)
T(10,N)=T(10,N-1)+4*REM2*(T(11,N-1)-T(10,N-1)+QT/PI/CON)
T(ML-2,N)=T(ML-2,N-1)+REM2*((TL-T(ML-2,N-1))*(X(NL-1)/P-.5*DX)-(T(
1ML-2,N-1)-T(ML-3,N-1))*(X(NL-1)-(P+.5)*DX))/((P+1)*X(NL-1)-DX*(.75
2*P**2+P+.25))
T(ML+1,N)=T(ML+1,N-1)+REM1*((T(ML+2,N-1)-T(ML+1,N-1))*(X(NL-1)+(3.
15-P)*DX)-(T(ML+1,N-1)-TL)*(X(NL-1)/(3-P)+.5*DX))/((4-P)*X(NL-1)+DX
2*(10-5.5*P+.75*P**2))
T(ML,N)=0
T(ML-1,N)=0
GO TO 700
500 MLP2=ML+2
T(ML,N)=0
T(ML-1,N)=0
EL=ML-10
T(ML+1,N)=T(ML+1,N-1)+REM1*((T(ML+2,N-1)-T(ML+1,N-1))*(X(NL-1)+(3.
15-P)*DX)-(T(ML+1,N-1)-TL)*(X(NL-1)/(3-P)+.5*DX))/((4-P)*X(NL-1)+DX
2*(10-5.5*P+.75*P**2))
DO 510 M=MLP2,KM1
G=M-10
510 T(M,N)=((1.-.5/G)*T(M-1,N-1)+(1.+5/G)*T(M+1,N-1))*REM1+(1.-2.*REM
11)*T(M,N-1)
T(10,N)=TL
DELTX=-DT*RRL/(X(NL-1)*DX)*(CON1*(T(ML+1,N-1)-TL)*(X(NL-1)/(3-P)+.
15*DX))
700 X(NL)=X(NL-1)+DELTX
ML=X(NL)/DX+10.99999999
P=(X(NL)+.5*DELTX)/DX-ML+12
IF (X(NL)) 710,710,800
710 DELTT=T(K,N-1)-T(10,N-1)
TOC=T(K,N-1)
DELTC=DELTT
CALL PLOTXY(TOC,DELTC,0,12)
TIME=DT*F
PRINT 720,TIME,DELTT,(T(JO,N-1),JO=10,K)
720 FORMAT(/40H THE TRANSITION IS COMPLETED AT TIME = F11.6,16H SECON
1DS. DELT=F12.7/12H TEMP = 10F12.7/11F12.7/10F12.7/10F12.7/)
T(11,N)=.33333333*(T(10,N)-T(13,N))+T(12,N)
P=0
DELTX=0
X(NL)=0
GO TO 800
750 DO 760 M=11,KM1
G=M-10
760 T(M,N)=((1.-.5/G)*T(M-1,N-1)+(1.+5/G)*T(M+1,N-1))*REM1+(1.-2.*REM
11)*T(M,N-1)
T(10,N)=T(10,N-1)+4*REM1*(T(11,N-1)-T(10,N-1)+QT/PI/CON)
IF(DELTS1-T(K,N-1)+T(10,N-1)+.0001) 800,950,950
800 CONTINUE
DELTT=T(K,INTER)-T(10,INTER)
TIME=DT*F
CALL PLOTXY(T(K,INTER),DELTT,1,0)

```

```

PRINT 820,TIME,DELTT,LL,X(NL),DELTX,ML,P,(T(JO,INTER),JO=10,K)
820 FORMAT(/6H TIME=F8.3,7H DELTT=F9.6,3H X(I4,2H)=F11.8,7H DELTX=F11.
18,4H ML=I3,3H P=F11.8/13H TEMPERATURE=10F12.7/1X11F12.7/1X10F12.7/
21X10F12.7)
X(10)=X(INTER)
DO 900 M=10,K
900 T(M,10)=T(M,INTER)
PRINT 920
920 FORMAT(/17H THE END IS HERE.)
IT=ITE
GO TO 999
950 DELTT=T(K,N)-T(10,N)
TIME=DT*F
PRINT 960,TIME,DELTT,(T(JO,N),JO=10,K)
960 FORMAT(/55H THE SHAPE OF THE PROFILE IS AGAIN INVARIANT AT TIME =
1F11.6,16H SECONDS DELTT=F12.7/12H TEMP = 10F12.7/11F12.7/10F1
22.7/10F12.7)
999 CONTINUE
CALL AXISXY(00,9,6,5.,150.,60.,0.,0.,0.,0.,1.,5)
1200 CONTINUE
WRITE(10,1300)
1300 FORMAT(9H /OSUEOF/)
CALL UNLOAD(10)
END

```

FINIS

'LOAD,56

'RUN,5

20	610	106	.08333333	.0125	.03175		
	.0163		.0146	.00589	.153	573.	
565.		565.	565.	565.	565.	565.	565.
565.		565.	565.	565.	565.	565.	
20	610	58	.16666666	.0125	.03175		
	.0163		.0146	.00589	.153	573.	
565.		565.	565.	565.	565.	565.	565.
565.		565.	565.	565.	565.	565.	
20	610	34	.33333333	.0125	.03175		
	.0163		.0146	.00589	.153	573.	
565.		565.	565.	565.	565.	565.	565.
565.		565.	565.	565.	565.	565.	

''

FORTTRAN Computer Program Employing  
Three-Point Finite Difference Equations

```

SEQUENCE,600,          CHEMICAL ENGINEERING      JOHN KAAKINEN
JOB,75038RMJK , JWK ,100,
FORTTRAN,L,X
PROGRAM INFCYL3
DIMENSION T(30,130),X(130)
READ 10,K,ITE,INTER,PHI,DT,DX,DIF1,DIF2,CON,RRL,TL,(T(M,10),M=10,K
1)
10 FORMAT(3I4,3F12.8/ 5F12.8/6F12.7/6F12.7/6F12.7/6F12.7/6F12.7/6F12.
17/6F12.7)
XT=DX*(K-10)
PHIM=60*PHI
REM1=DT*DIF1/DX**2      $REM2=DT*DIF2/DX**2
EM1=1/REM1      $ EM2=1/REM2
PRINT 20,K,ITE,INTER,PHI,PHIM,DT,DX,DIF1,DIF2,EM1,EM2,TL,XT,CON,RR
1L,(T(M,10),M=10,K)
20 FORMAT(50X,4HDATA/4H K=I4,5H ITE=I4,7H INTER=I4,5H PHI=F9.6,8HDEG
1/SEC=F6.2,12HDEG/MIN DT=F10.8,4H DX=F10.8/7H DIF1=F12.8,6H DIF2=
2F12.8,4H M1=F12.8,4H M2=F12.8,4H TL=F6.2,4H XT=F6.4,5H CON=F8.4,5H
2 RRL=F8.4/36H THE INITIAL TEMPERATURE PROFILE = 7F12.7/10F12.7/10
1F12.7/10F12.7/4F12.7)
DELTS1=.25*PHI*XT**2/DIF1  $ DELTS2=.25*PHI*XT**2/DIF2
DELTA=22.3*PHI*XT**2
PRINT 30,DELTS1,DELTS2,DELTA
30 FORMAT(/9H DELTS1=F12.7,9H DELTS2=F12.7,8H DELTA=F12.7//)
DO 35 L=10,INTER
35 X(L)=XT
CON1=CON2=CON
TK0=T(K,10)
KEY=-1
KM1=K-1  $ KM2=K-2  $ KM3=K-3  $ KM4=K-4
P=ML=DELTX=LL=0
MLO=K
DO 900 IT=11,ITE
DO 800 N=11,INTER
F=N+(IT-11)*(INTER-10)-10
T(K,N)=PHI*DT*F+TK0
NL=N
IF(X(NL)) 750,750,40
40 IF(TL-T(K,N)) 100,100,50
50 DO 60 M=11,KM1
G=M-10
60 T(M,N)=((1.-.5/G)*T(M-1,N-1)+(1.+.5/G)*T(M+1,N-1))*REM2+(1.-2.*REM
12)*T(M,N-1)
T(10,N)=T(10,N-1)+4*REM2*(T(11,N-1)-T(10,N-1))
GO TO 800
100 IF (KEY) 110,110,199

```

```

110 TIME=DT*(F-1)
    DELTT=T(K,N-1)-T(10,N-1)
    PRINT 120,TIME,DELTT,(T(JO,N-1),JO=10,K)
120 FORMAT(/55H THE TRANSITION IS BEGINNING AT THE SURFACE AT TIME =
1F11.6,16H SECONDS DELTT=F12.7/12H TEMP = 10F12.7/11F12.7/10F1
22.7/10F12.7)
    P=2
    ML=K
    KEY=1
    ENLD=F-1
199 LL=F-ENLD
    GO TO (200,300,350,400),K-ML+1
200 DELTX=DT*RRL*CON2*.5/DX*((2*P+1)/(P*(P+1))*TL-(P+1)/P*T(K-2,N-1)+P
1/(P+1)*T(K-3,N-1))-X(NL-1)+XT-SQRT((((2*P+1)/(P*(P+1))*TL-(P+1)/P*
2T(K-2,N-1)+P/(P+1)*T(K-3,N-1))*CON2*RRL*.5*DT/DX-X(NL-1)+XT)**2+((
32*P+1)/(P*(P+1))*TL-(P+1)/P*T(K-2,N-1)+P/(P+1)*T(K-3,N-1))*2*DT*CO
4N2*RRL/DX*(X(NL-1)-XT)+DT**2*CON1*RRL/X(NL-1)*(XT+X(NL-1))*PHI*(NL
5-10.5))
    DO 210 M=11,KM3
    G=M-10
210 T(M,N)=((1.-.5/G)*T(M-1,N-1)+(1.+5/G)*T(M+1,N-1))*REM2+(1.-2.*REM
12)*T(M,N-1)
    T(10,N)=T(10,N-1)+4*REM2*(T(11,N-1)-T(10,N-1))
    T(ML-1,N)=0
    EL=ML-10
    T(ML-2,N)=T(ML-2,N-1)+REM2*((EL-2+P)/((EL-2)*(P+1)*P)*((2*P+1)/(P*
1(P+1))*TL-(P+1)/P*T(ML-2,N-1)+P/(P+1)*T(ML-3,N-1)))+(P-1)/P*(1/(P*(
2P+1))*TL+(P-1)/P*T(ML-2,N-1)-P/(P+1)*T(ML-3,N-1))-P/(P+1)*(EL-3)/(
3EL-2)*(-1/(P*(P+1))*TL+(P+1)/P*T(ML-2,N-1)-(P+2)/(P+1)*T(ML-3,N-1)
4))
    GO TO 700
300 DELTX=DT*RRL/X(NL-1)*(-CON1*(XT+X(NL-1))*5*PHI*DT*(NL-1)/(XT-X(N
1L-1))+CON2*X(NL-1)/DX*((2*P+1)/(P*(P+1))*TL-(P+1)/P*T(K-3,N-1)+P/(
2P+1)*T(K-4,N-1)))
    DO 310 M=11,KM4
    G=M-10
310 T(M,N)=((1.-.5/G)*T(M-1,N-1)+(1.+5/G)*T(M+1,N-1))*REM2+(1.-2.*REM
12)*T(M,N-1)
    T(10,N)=T(10,N-1)+4*REM2*(T(11,N-1)-T(10,N-1))
    T(ML,N)=0
    T(ML-1,N)=0
    EL=ML-10
    T(ML-2,N)=T(ML-2,N-1)+REM2*((EL-2+P)/((EL-2)*(P+1)*P)*((2*P+1)/(P*
1(P+1))*TL-(P+1)/P*T(ML-2,N-1)+P/(P+1)*T(ML-3,N-1)))+(P-1)/P*(1/(P*(
2P+1))*TL+(P-1)/P*T(ML-2,N-1)-P/(P+1)*T(ML-3,N-1))-P/(P+1)*(EL-3)/(
3EL-2)*(-1/(P*(P+1))*TL+(P+1)/P*T(ML-2,N-1)-(P+2)/(P+1)*T(ML-3,N-1)
4))
    GO TO 700
350 IF (ML-ML0) 370,420,420
370 T(K-1,N-1)=(TL+T(K,N-1)*(3-P))/(4-P)
    GO TO 415
400 IF (ML-ML0) 410,420,420
410 T(ML+1,N-1)=(P-3)/(5-P)*T(ML+3,N-1)+2*(P-3)/(P-4)*T(ML+2,N-1)+2/((
1P-5)*(P-4))*TL
415 ML0=ML
420 GO TO (750,500,500,430),ML-9
430 DELTX=DT*RRL*(-CON1/DX*((P-3)/(4-P)*T(ML+2,N-1)+(P-4)/(P-3)*T(ML+1
1,N-1)+(2*P-7)/((P-3)*(P-4))*TL)+CON2/DX*((2*P+1)/(P*(P+1))*TL-(P+1
2)/P*T(ML-2,N-1)+P/(P+1)*T(ML-3,N-1)))
    EL=ML-10

```

```

T(ML-2,N)=T(ML-2,N-1)+REM2*((EL-2+P)/((EL-2)*(P+1)*P)*((2*P+1)/(P*
1*(P+1))*TL-(P+1)/P*T(ML-2,N-1)+P/(P+1)*T(ML-3,N-1))+P-1)/P*(1/(P*(
2*P+1))*TL+(P-1)/P*T(ML-2,N-1)-P/(P+1)*T(ML-3,N-1))-P/(P+1)*(EL-3)/(
3EL-2)*(-1/(P*(P+1))*TL+(P+1)/P*T(ML-2,N-1)-(P+2)/(P+1)*T(ML-3,N-1)
4))
T(ML+1,N)=T(ML+1,N-1)+REM1*((3-P)*(EL+2)/((4-P)*(EL+1))*((5-P)/(4-
1P)*T(ML+2,N-1)+(4-P)/(P-3)*T(ML+1,N-1)+1/((P-3)*(P-4))*TL)+(2-P)/(
2P-3)*((3-P)/(4-P)*T(ML+2,N-1)+(P-2)/(3-P)*T(ML+1,N-1)-1/((P-4)*(P-
33))*TL)-(EL-2+P)/((P-3)*(P-4)*(EL+1))*((P-3)/(4-P)*T(ML+2,N-1)+(4-
4P)/(3-P)*T(ML+1,N-1)+(2*P-7)/((P-4)*(P-3))*TL))
T(ML,N)=0
T(ML-1,N)=0
MLP2=ML+2
DO 460 M=MLP2,KM1
G=M-10
460 T(M,N)=((1.-.5/G)*T(M-1,N-1)+(1.+5/G)*T(M+1,N-1))*REM1+(1.-2.*REM
11)*T(M,N-1)
MLM3=ML-3
DO 470 M=11,MLM3
G=M-10
470 T(M,N)=((1.-.5/G)*T(M-1,N-1)+(1.+5/G)*T(M+1,N-1))*REM2+(1.-2.*REM
12)*T(M,N-1)
T(10,N)=T(10,N-1)+4*REM2*(T(11,N-1)-T(10,N-1))
GO TO 700
500 MLP2=ML+2
T(ML,N)=0
T(ML-1,N)=0
EL=ML-10
T(ML+1,N)=T(ML+1,N-1)+REM1*((3-P)*(EL+2)/((4-P)*(EL+1))*((5-P)/(4-
1P)*T(ML+2,N-1)+(4-P)/(P-3)*T(ML+1,N-1)+1/((P-3)*(P-4))*TL)+(2-P)/(
2P-3)*((3-P)/(4-P)*T(ML+2,N-1)+(P-2)/(3-P)*T(ML+1,N-1)-1/((P-4)*(P-
33))*TL)-(EL-2+P)/((P-3)*(P-4)*(EL+1))*((P-3)/(4-P)*T(ML+2,N-1)+(4-
4P)/(3-P)*T(ML+1,N-1)+(2*P-7)/((P-4)*(P-3))*TL))
DO 510 M=MLP2,KM1
G=M-10
510 T(M,N)=((1.-.5/G)*T(M-1,N-1)+(1.+5/G)*T(M+1,N-1))*REM1+(1.-2.*REM
11)*T(M,N-1)
T(10,N)=TL
IF (X(NL-1)-.2*DX) 550,550,530
530 DELTX=DT*RRL*(-CON1/DX*((P-3)/(4-P)*T(ML+2,N-1)+(P-4)/(P-3)*T(ML+1
1,N-1)+(2*P-7)/((P-3)*(P-4))*TL)+CON2*.5*(TL-T(10,N-1))/X(NL-1))
T(10,N)=T(10,N-1)+4*(DX/X(NL-1))*2*REM2*(TL-T(10,N-1))
GO TO 700
550 DELTX=DT*RRL*(-CON1/DX*((P-3)/(4-P)*T(ML+2,N-1)+(P-4)/(P-3)*T(ML+1
1,N-1)+(2*P-7)/((P-3)*(P-4))*TL))
700 X(NL)=X(NL-1)+DELTX
ML=X(NL)/DX+10.99999999
P=X(NL)/DX-ML+12
IF (X(NL)) 710,710,800
710 DELTT=T(K,N-1)-T(10,N-1)
TOC=T(K,N-1)
DELTC=DELTT
TIME=DT*F
PRINT 720,TIME,DELTT,(T(JO,N-1),JO=10,K)
720 FORMAT(/40H THE TRANSITION IS COMPLETED AT TIME = F11.6,16H SECON
1DS. DELT=F12.7/12H TEMP = 10F12.7/11F12.7/10F12.7/10F12.7/)
T(11,N)=.33333333*(T(10,N)-T(13,N))+T(12,N)
P=0
DELTX=0
X(NL)=0

```

```

GO TO 800
750 DO 760 M=11,KM1
    G=M-10
760 T(M,N)=((1.-.5/G)*T(M-1,N-1)+(1.+5/G)*T(M+1,N-1))*REM1+(1.-2.*REM
    11)*T(M,N-1)
    T(10,N)=T(10,N-1)+4*REM1*(T(11,N-1)-T(10,N-1))
    IF(DELT(S1-T(K,N-1)+T(10,N-1)+.0001) 800,950,950)
800 CONTINUE
    DELTT=T(K,INTER)-T(10,INTER)
    TIME = DT*F
    PRINT 820,TIME,DELTT,LL,X(NL),DELTX,ML,P,(T(JO,INTER),JO=10,K)
820 FORMAT(/6H TIME=F8.3,7H DELTT=F9.6,3H X(14,2H)=F11.8,7H DELTX=F11.
    18,4H ML=I3,3H P=F11.8/13H TEMPERATURE=10F12.7/1X11F12.7/1X10F12.7/
    21X10F12.7)
    X(10)=X(INTER)
    DO 900 M=10,K
900 T(M,10)=T(M,INTER)
    PRINT 920
920 FORMAT(/17H THE END IS HERE.)
    IT=ITE
    GO TO 999
950 DELTT=T(K,N)-T(10,N)
    TIME=DT*F
    PRINT 960,TIME,DELTT,(T(JO,N),JO=10,K)
960 FORMAT(/55H THE SHAPE OF THE PROFILE IS AGAIN INVARIANT AT TIME =
    1F11.6,16H SECONDS DELTT=F12.7/12H TEMP = 10F12.7/11F12.7/10F1
    22.7/10F12.7)
999 CONTINUE
    END

```

FINIS

'LOAD,56

'RUN,5

208610	130	.33333333	.00125	.03175		
.00163		.00146	.000589	.153	573.	
565.	565.	565.	565.	565.	565.	565.
565.	565.	565.	565.	565.	565.	

''